TNO report
PML 1996-A76

Dynamic deformation capacity of reinforced concrete
Phase 4: Influence of shear reinforcement

TNO Prins Maurits Laboratory

Lange Kleiweg 137
P.O. Box 45
2280 AA Rijswijk
The Netherlands

Phone +31 15 284 28 42
Fax +31 15 284 39 58

Date
January 1997

Author(s)
J.C.A.M. van Doormaal

Classification

Classified by	:	D. Boon
Classification date	:	January 9, 1997

Title	:	Ongerubriceerd
Managementuittreksel	:	Ongerubriceerd
Abstract	:	Ongerubriceerd
Report text	:	Ongerubriceerd
Annexes A - E	:	Ongerubriceerd

Copy no.	:	13	
No. of copies	:	26	
No. of pages	:	72	(incl. annexes, excl. RDP & distribution list)
No. of annexes	:	5	

All information which is classified according to Dutch regulations shall be treated by the recipient in the same way as classified information of corresponding value in his own country. No part of this information will be disclosed to any party.

The classification designation Ongerubriceerd is equivalent to Unclassified.

TNO Prins Maurits Laboratory is part of
TNO Defence Research which further consists of:

TNO Physics and Electronics Laboratory
TNO Human Factors Research Institute

Netherlands Organization for
Applied Scientific Research (TNO)

DISCLAIMER NOTICE

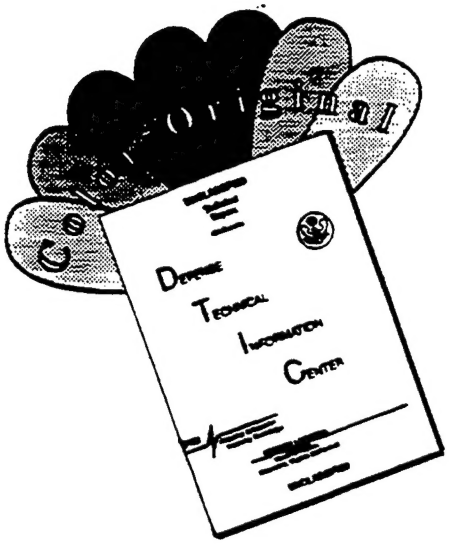

THIS DOCUMENT IS BEST QUALITY AVAILABLE. THE COPY FURNISHED TO DTIC CONTAINED A SIGNIFICANT NUMBER OF COLOR PAGES WHICH DO NOT REPRODUCE LEGIBLY ON BLACK AND WHITE MICROFICHE.

Managementuittreksel

Titel	:	Dynamic deformation capacity of reinforced concrete Phase 4: Influence of shear reinforcement
Auteur(s)	:	Ir. J.C.A.M. van Doormaal
Datum	:	januari 1997
Opdrachtnr.	:	A96D449
Rapportnr.	:	PML 1996-A76

Achtergrond
Op verzoek van MoD/DGW&T/CD/TB zijn schokgolf-experimenten uitgevoerd op opgelegde platen van gewapend beton. Tijdens deze experimenten is de volledige weerstand-vervormingskarakteristiek van de geteste platen bepaald, dat wil zeggen tot en met falen van de plaat. De aandacht ging met name uit naar de dynamische vervormingscapaciteit van het gewapende beton en naar de invloed hierop van de verbindingswapening (beugels en veterwapening).
De huidige proevenserie is een vervolg op eerdere experimenten ([1] en [2]), waarin eveneens de dynamische vervormingscapaciteit van gewapend beton het onderwerp van onderzoek was.

De aanleiding om onderzoek te doen naar deze grootheid was de observatie dat in ontwerpschriften vaak conservatieve waarden voor de toelaatbare vervorming van gewapend beton worden voorgeschreven. Conservatisme is uiteraard onvermijdelijk voor ontwerpvoorschriften, die algemeen toepasbaar moeten zijn. Maar aan het conservatieve karakter van de voorschriften ten aanzien van de toelaatbare vervorming van gewapend beton lijkt ook een hiaat in kennis ten grondslag te liggen. Dit betekent dat beschermingsconstructies vaak economischer ontworpen kunnen worden of dat beschermingsconstructies een hoger beschermingsgraad hebben dan wordt aangenomen. Om deze wetenschap ten voordele aan te kunnen wenden, is een beter begrip ten aanzien van de dynamische vervormingscapaciteit en de invloedsparameters nodig.

De voorgaande experimenten hebben waardevolle resultaten opgeleverd. Het bleek mogelijk om een empirische relatie te formuleren tussen de testparameters en de vervormingscapaciteit van de plaat. Omdat deze empirische relatie gebaseerd is op een beperkt aantal experimenten is validatie ervan nog wel nodig. Verder is hij slechts toepasbaar voor een kleine categorie platen met dezelfde parameters als de geteste platen. Dat zijn de redenen voor de huidige serie testen: verificatie van eerdere resultaten en uitbreiding van de kennis over de dynamische vervormingscapaciteit van gewapend beton door andere parameters mee te nemen. Als extra parameter is in de huidige serie de verbindingswapening in beschouwing genomen.

De doelstelling van de huidige serie experimenten is:

- verificatie van de empirische relatie;
- invloed van de verbindingswapening op de deformatiecapaciteit van gewapend beton;
- meer data over de respons van gewapend beton onder een schokgolf.

Experimenten

Een zevental schokgolfproeven is uitgevoerd in de blastsimulator van het TNO Prins Maurits Laboratorium (TNO-PML) op een drietal verschillende typen betonplaten, zonder verbindingswapening, met beugels of met veterwapening. De wijze van bevestiging van de platen kan beschouwd worden als een vrije oplegging. De platen waren in langsrichting allen op dezelfde manier gewapend met een wapeningspercentage van 0,48%. Verdere gegevens over de platen zijn: lengte: 1,20 m; ondersteunde lengte: 1,10 m; breedte: 0,85 m en dikte: 80 mm.

Resultaten

De weerstand-vervormingscurves van de platen zijn het resultaat van de experimenten. Uit deze curves kan de vervormingscapaciteit van de platen afgelezen worden, behalve voor de platen met veterwapening. Die faalden op een moment dat de respons van de plaat niet meer geregistreerd werd.
De weerstand-vervormingscurves leidden tot de volgende observaties en conclusies.

- De resultaten voor de platen zonder afschuifwapening sluiten aan bij voorgaande resultaten. De resultaten ondersteunen de empirische relatie die eerder al was gevonden.
- De deformatiecapaciteit van de platen met beugels was slechts een weinig groter dan die van de platen zonder beugels.
- De veterwapening heeft een behoorlijke invloed op de deformatiecapaciteit. Helaas kon deze invloed niet goed gekwantificeerd worden.
- De vervormingscapaciteit onder meerdere schokgolven blijkt geringer te zijn. Dergelijke experimenten leveren dus een ondergrens voor de dynamische vervormingscapaciteit onder een enkele schokgolf.
- Voor de platen zonder bindingswapening waren de voorschriften van TM 5-1300 behoorlijk conservatief (factor 2). Voor de platen met beugels was TM 5-1300 slechts in geringe mate conservatief. Voor de platen met veterwapening geeft TM 5-1300 daarentegen een veel grotere vervorming als toelaatbaar dan wat de platen bereikten. Hieruit blijkt dus dat voorzichtigheid in het gebruik van TM 5-1300 geboden is. De meest logische verklaring voor de ongunstige resultaten van de platen met veterwapening is dat in slanke platen de vervorming sterk gelokaliseerd wordt door de bindende werking van de veterwapening.

Voortgang

Voor de vervolgfase wordt voorgesteld dikkere platen te testen. Daarmee kan de bovengenoemde hypothese ten aanzien van de werking van veterwapening gecon-

troleerd worden. Voor het vertrouwen in ontwerpen op basis van TM 5-1300 is dit nodig. Verder kan met de testen de validiteit van de empirische relatie ofwel uitgebreid ofwel beter afgebakend worden.

Contents

1 Introduction

At the request of MoD/DGW&T/CD/TB blast experiments were carried out on simply supported reinforced concrete slabs in order to determine their resistance-deformation characteristic up to failure. The main interest was the dynamic rotation capacity of the slabs and the influence of binding reinforcement on this rotation capacity.
The present test series is a sequel to previous test series ([1] and [2]) in which the dynamic rotation capacity of reinforced concrete slabs was also the main subject. The interest in this parameter has been raised by the observation that in design rules, often conservative values are used for the maximum deformation capacity of reinforced concrete (see [3]). That means that the design of protective structures in many cases can be more economical or the protection level of a structure is higher than assumed. In order to be able to turn this knowledge to profit, a better understanding of the dynamic deformation capacity and of the parameters of influence is needed.

The previous tests have given valuable results. It appeared to be possible to formulate an empirical relationship between the test parameters and the deformation capacity of the slab. Since this empirical relationship is only based on a limited number of tests, its applicability is only limited. Furthermore, it needs some more validation. That is why the present series of tests has been performed, to verify the generalised result of the previous tests and to extend the knowledge on dynamic deformation capacity of reinforced concrete by taking other parameters into account.
The objectives of the present test series were:

- verification of the empirical relationship;
- influence of binding reinforcement on the deformation capacity of reinforced concrete;
- more data on the response of reinforced concrete slabs under a shock wave.

In this report the experiments and the results are described. In Chapter 2, the experimental programme is given. All data on the slabs is presented in this chapter. Furthermore, it describes what is measured during the tests.
Chapter 3 gives the results of each slab tested in the present programme. The behaviour of each slab is described with the use of the resistance-deformation curve, which could be obtained from the measurements.
In Chapter 4, the results of the slabs are compared with each other and with the results of the previous test programme. They are also compared with calculations according to TM 5-1300 [4], a manual which is often used for the design of protective structures.
The report ends with Chapter 5, which gives all the conclusions of the research project.

2 Experimental programme

2.1 Introduction

The slabs in the present programme were tested in the same set-up as in the previous programmes, that means in the blast simulator at TNO Prins Maurits Laboratory (TNO-PML).
The main differences between the present programme and the previous ones concern the type of reinforcement of the slabs, and the number of shocks by which the slabs will be brought to failure.
An overview of the test programme is given in this chapter. For a description of the principle of the test method and the fixation of the slab such that a simple support is realised, one is referred to [1].

2.2 The slabs

The primary objective of the test programme was to find out what influence the type of shear reinforcement has on the deformation capacity of reinforced concrete. Therefore it was decided to test three different types of slabs, with three different types of shear reinforcement; none, stirrups and lacing.
The three slabs without tying reinforcement were to be brought to failure by a different number of shocks, in order to find out whether the deformation capacity changes with the number of shocks. In the previous test series, some slabs could not be brought to failure by a single shock. The capacity of the blast simulator was too limited. That is why these slabs were brought to failure by two or three shocks. The present test series on the three slabs without tying reinforcement should show whether it was correct to assume that the deformation at failure does not depend much on the number of shocks.
The two slabs with stirrups and the two with lacing were planned to fail under the minimum number of shocks possible.
Since it was not possible to predict what part of energy in the shock wave would be converted into kinetic energy of the rigid motion of the slab and what part into deformation energy of the slab, we just had to make a try with the amount of oxygen-gas mixture to be used in the tests. The test programme turned out to be as given in Table 2.1.

Table 2.1: Test programme.

Slab	Number of shocks	Amount of oxygen-gas mixture in subsequent tests (litre)
1	1	95
2	5	50 - 50 - 50 - 60 - 70
3	2	70 - 70
4	1	110
5	1	110
6	1	110
7	1	110

In Table 2.2, all data on the dimensions of the slabs and the material properties are presented. One is referred to Annex B for more information about the concrete properties. In Figures 2.1 and 2.2, all data on the reinforcement, with details about the stirrups and the lacing, are given.

Table 2.2: Data on tested slabs.

	Slab type 3.1 no tying reinforcement numbers 1-3	Slab type 3.2 with stirrups numbers 4-5	Slab type 3.3 with lacing numbers 6-7
Dimensions of slabs			
Length L [m]	1.2	1.2	1.2
Support length L_s [m]	1.1	1.1	1.1
Width W [m]	0.85	0.85	0.85
Height H [m]	0.08	0.08	0.08
Mass M_{tot} [kg]	213.56	213.56	213.56
Reinforcement			
Diameter [mm]	6	6	6
In-between distance b [mm]	92.5	92.5	92.5
Concrete cover c [mm]	12	12	15
Number of rods n	9	9	9
Ratio [%]	0.483	0.483	0.483
Properties of concrete			
Cube strength f_c [MPa]	42.5	39.2	39.2
Young' s modulus E_c [GPa]	26.1	27.1	27.1
Poisson's ratio	0.2	0.2	0.2
Properties of steel (specification of manufacturer)			
Yield strength f_y [MPa]	500	500	500
Ultimate strength f_u [MPa]	580	580	580
Young's modulus E_s [GPa]	210	210	210

The slabs were 80 mm thick. That is inbetween the thickness of the slabs of the previous two series. The choice of this thickness is based on the requirement that failure in one shock should be possible.

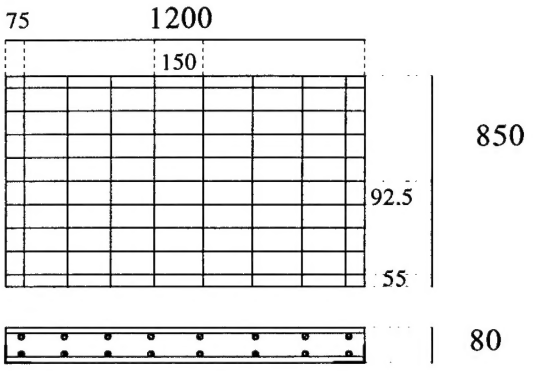

Concrete cover: 12 mm
Diameter reinforcement: 6 mm

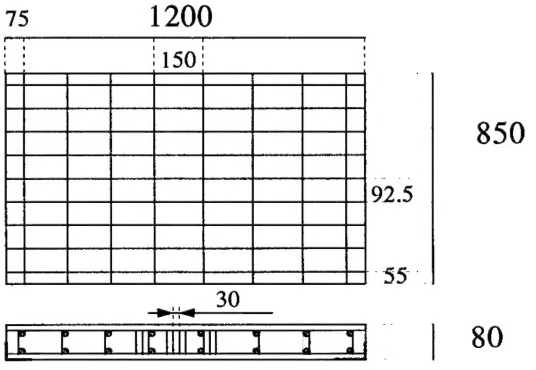

Concrete cover: 12 mm
Diameter reinforcement: 6 mm
stirrups: 3 mm

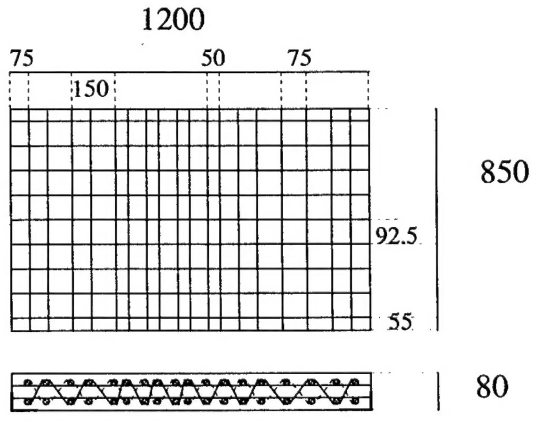

Concrete cover: 15 mm
Diameter reinforcement: 6 mm in longitudinal direction
4 mm in transverse direction
lacing: 3 mm

Figure 2.1: The three different types of slabs.

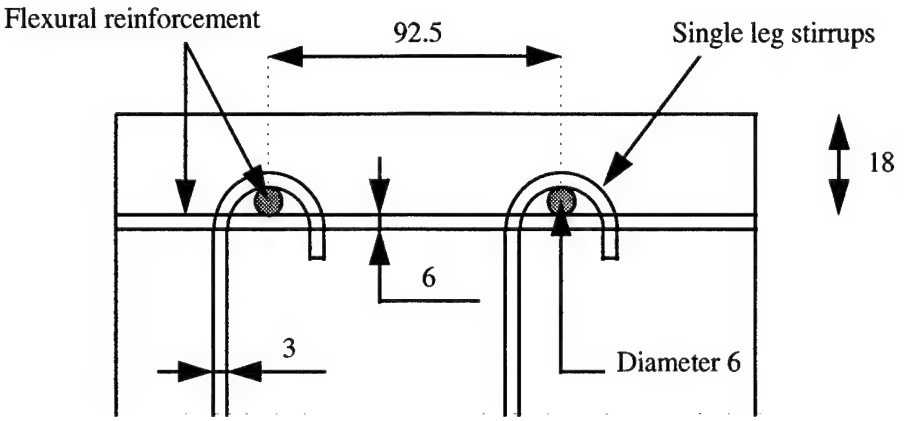

a- slab type 3.2: with stirrups.
Dimensions in mm.

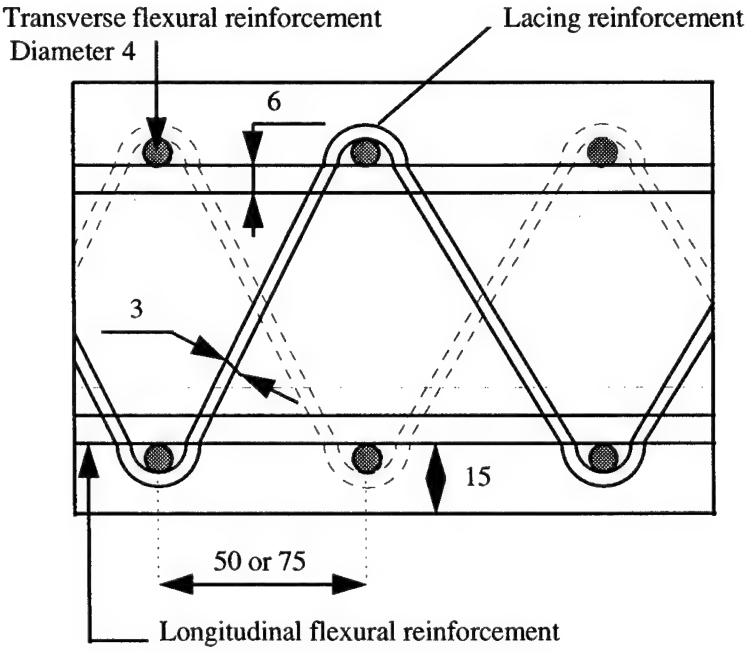

b- slab type 3.3: with lacing.
Dimensions in mm.

Figure 2.2: Stirrups and lacing.

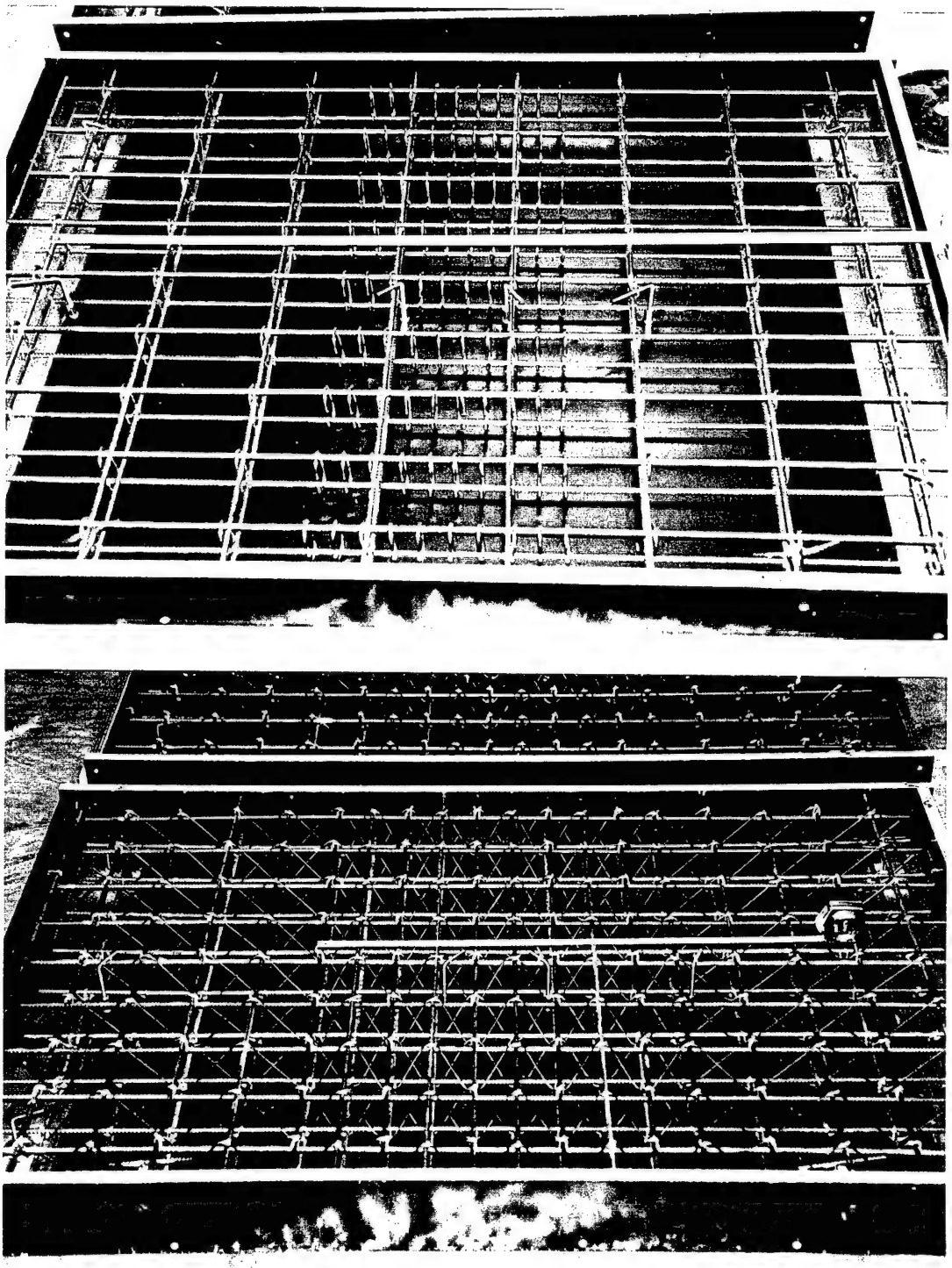

Figure 2.3: Stirrups and lacing.

2.3 Measurements

The blast pressure was measured on the mask, just underneath the slab, using a Druck Miniature Semiconductor Pressure Transducer Type PDCR 200. Since it is known that the load is uniformly distributed, this single measurement for the pressure is sufficient. Additionally the incident pressure was measured at a distance of 1.5 m in front of the slab.
Both the displacement and acceleration were measured at four different locations along the centre line of the slab. These positions are given in Figure 2.4. The displacement was measured using contactless laser sensors, Micro-Epsilon model LD 1605. The acceleration was measured with either a Hottinger B12/2000 (A1, A3 and A4) or an ENDEVCO 2262 (A2).

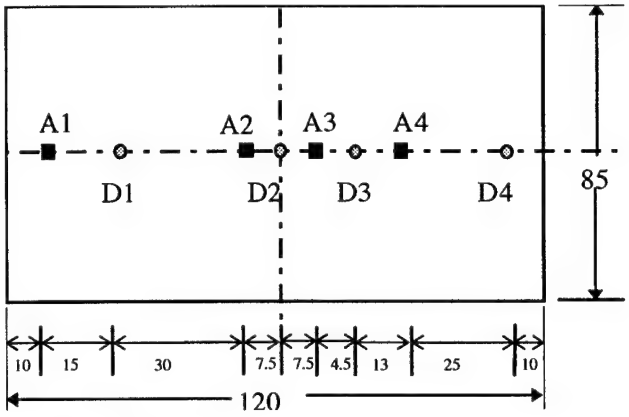

Figure 2.4: Locations of measurement, co-ordinates in cm.

3 Results

3.1 Introduction

In this chapter, the results of the tests are presented. The procedure to derive the resistance-deformation curve from the measured signals is described in Annex C. These curves are only presented here.
A remark is needed on the accelerations measured at locations A2 and A3. These points of measurement are symmetrically located on the slab, so they should give, the same signal for the slabs that failed in the centre. In all tests, however, we have noticed that A2 and A3 differed a little from each other. This difference does not indicate that one of the measurements is incorrect. It is due to the fact that two different transducers are used at the two locations, each with its own damping characteristics. Changing the filtering frequency for the signals shows that the difference has to do with a different number of frequencies in the signals. A change in the filtering frequency changes also the difference between the two acceleration signals. Both signals are used in the analysis of the response of the slabs.

3.2 Slab 1

The test on this slab was performed on March 28th, 1996. The slab was loaded by a shock wave generated by 95 litres of oxygen-acetylene mixture with a mass ratio of 1 - 1. It failed after one shock, and the failure crack was located at position A3. The asymmetric failure can be explained by the fact that there is no transverse reinforcement in the centre of the slab, and that there are two bars at each side of the centre, at A2 and A3. As explained in previous tests (see [1]), the slab failed on a transverse reinforcement bar because of a stress concentration in the concrete at such a position.
The global crack pattern is sketched in Figure 3.1. Cracks were first formed symmetrically at D2 (at the centre of the slab) and at A2 and A3. Then it appeared that the failure had occurred on one of the two cracks already formed, by chance.
Figure 3.2 shows the real crack pattern.

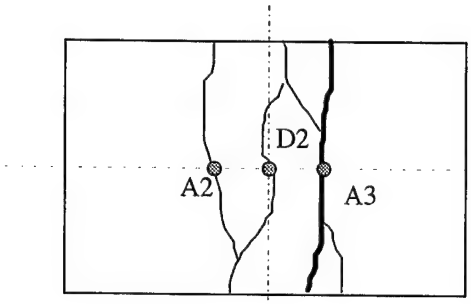

Figure 3.1: Global crack pattern in slab 1.

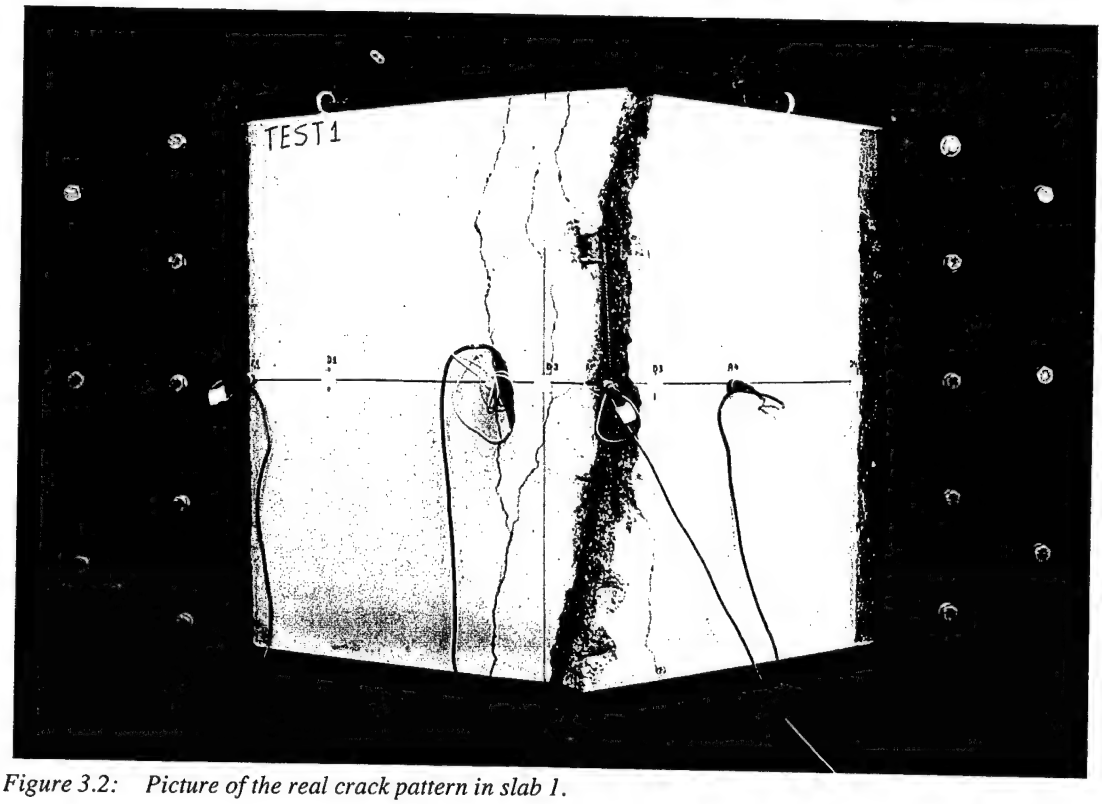

Figure 3.2: Picture of the real crack pattern in slab 1.

Figure 3.3 shows the resistance-deformation curve of the slab. The deformation in this curve represents the deflection at the failure point of the slab. This result is obtained by splitting up the motion of the slab into a contribution of rigid motion and a contribution of bending motion. The contribution of rigid motion is eliminated to leave only the bending motion. The shape functions used and the way this curve is obtained are given in Annex C.

From this curve, it can be seen that the maximum resistance of the slab is about 88 kN. The permanent deflection at failure is 41 mm, which corresponds with a support rotation of 3.7° for the left support, and of 5.0° for the right support, so an average support rotation of 4.4°.

The energy absorbed by the slab is equal to the surface underneath the resistance-deformation curve and has been calculated to be 3.3 kJ.

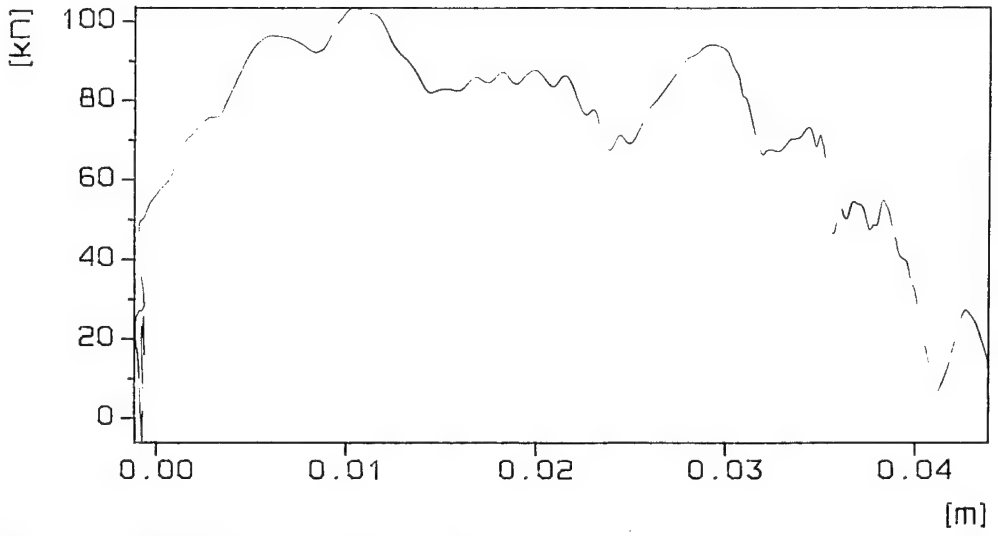

Figure 3.3: Resistance-deformation curve of slab 1.

3.3 Slab 2

The tests on this slab were performed on March 29th, 1996. The slab was loaded by five subsequent shock waves, respectively generated by 50, 50, 50, 60 and 70 litres of oxygen-acetylene mixture with a mass ratio of 1 - 1. It failed after the fifth shock, and the failure crack was located at A2.
The global crack pattern is sketched after each of the five tests. They are shown in Figure 3.4. Cracks were first formed symmetrically at D2 (at the centre of the slab) and at A2 and A3. After the last test it appeared that failure had occurred on one of the two cracks already formed alongside the centre, by chance. Figure 3.5 shows the real crack pattern after the fourth and fifth test.

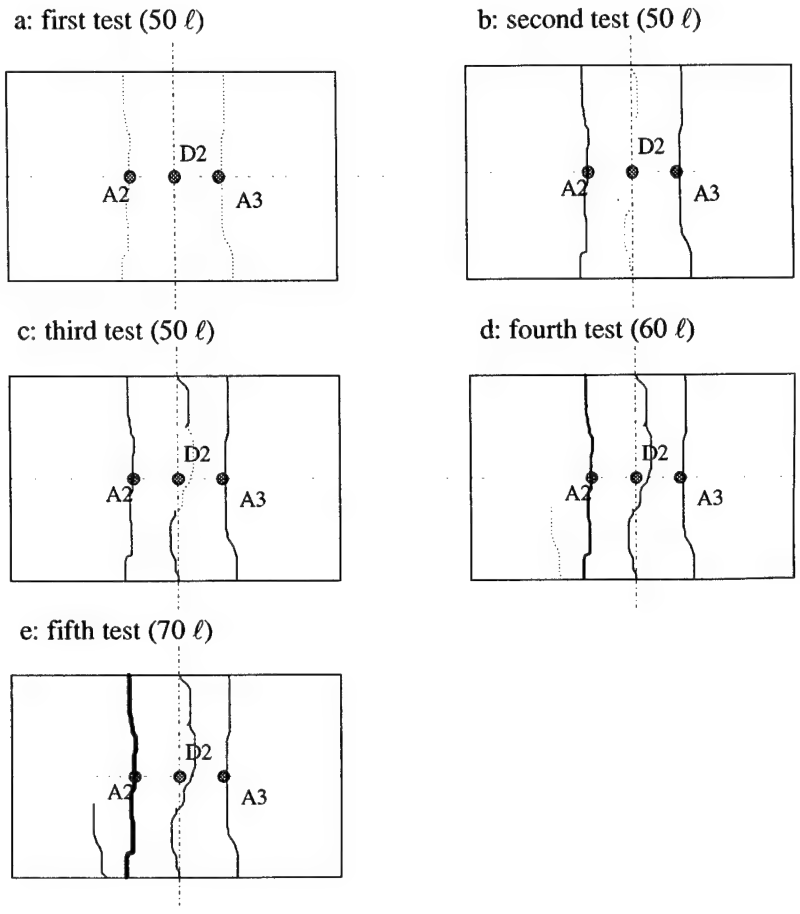

Figure 3.4: Global crack pattern in slab 2.
a: after first test; b: after second test;
c: after third test; d: after fourth test;
e: after fifth test.

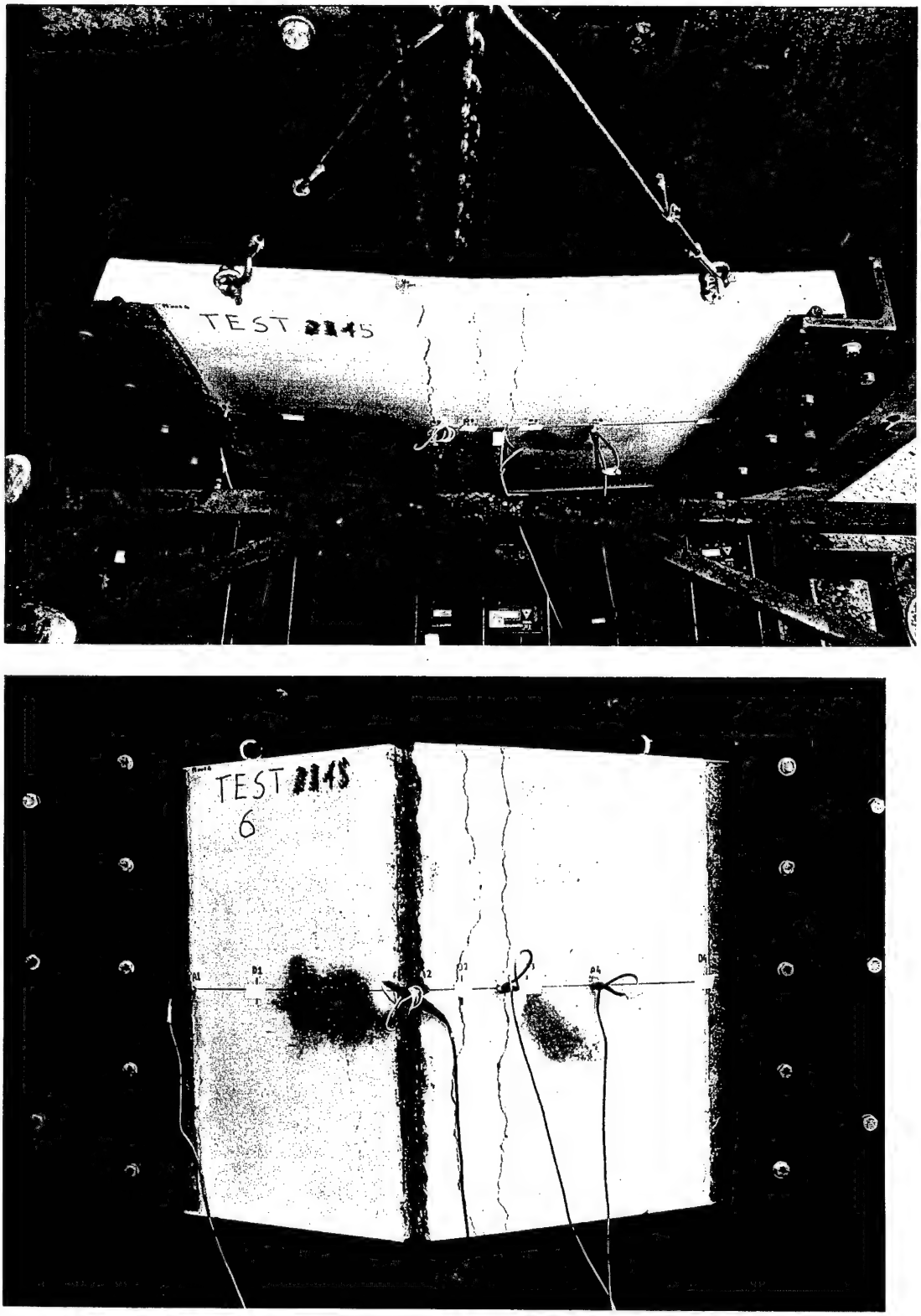

Figure 3.5: Pictures of the real crack pattern in slab 2.
a: test 5; b: test 6.

Figure 3.6 shows the resistance-deformation curve of the slab, for each test. The deformation in this curve represents the deflection at the centre of the slab for tests 1 to 4, and at the failure point A2 for test 5.
In the elastic phase, the global response of the slab is disturbed by higher frequency modes. Therefore the deflection in the centre of the slab is initially negative (see the deformation shapes in Annex D). The ascending branch of the resistance-deformation curve is therefore not correct.

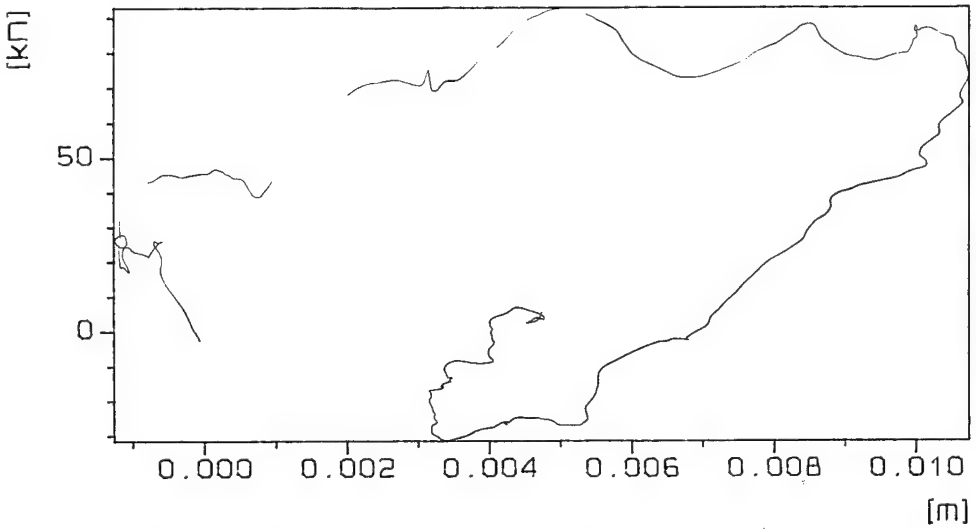

Figure 3.6a: Resistance-deformation curve of slab 2 - first test.

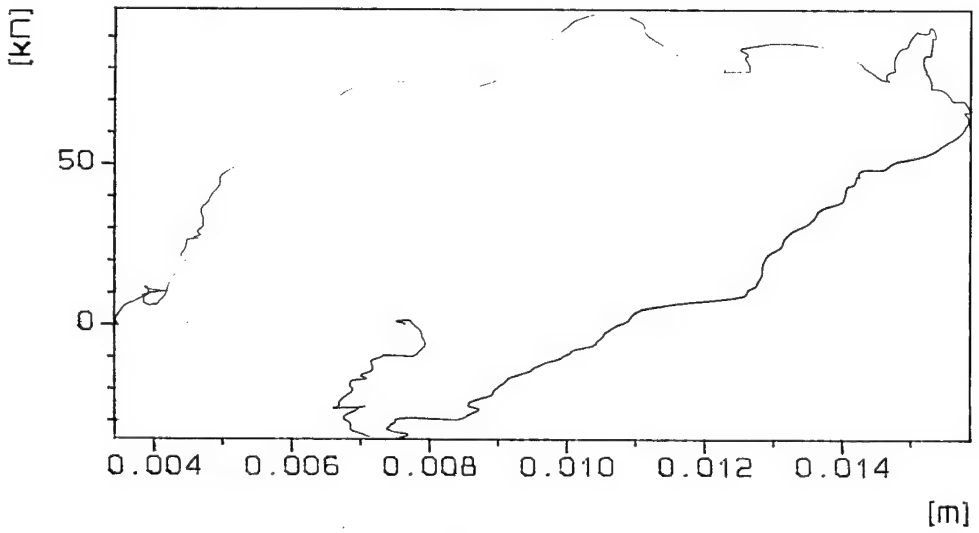

Figure 3.6b: Resistance-deformation curve of slab 2 - second test.

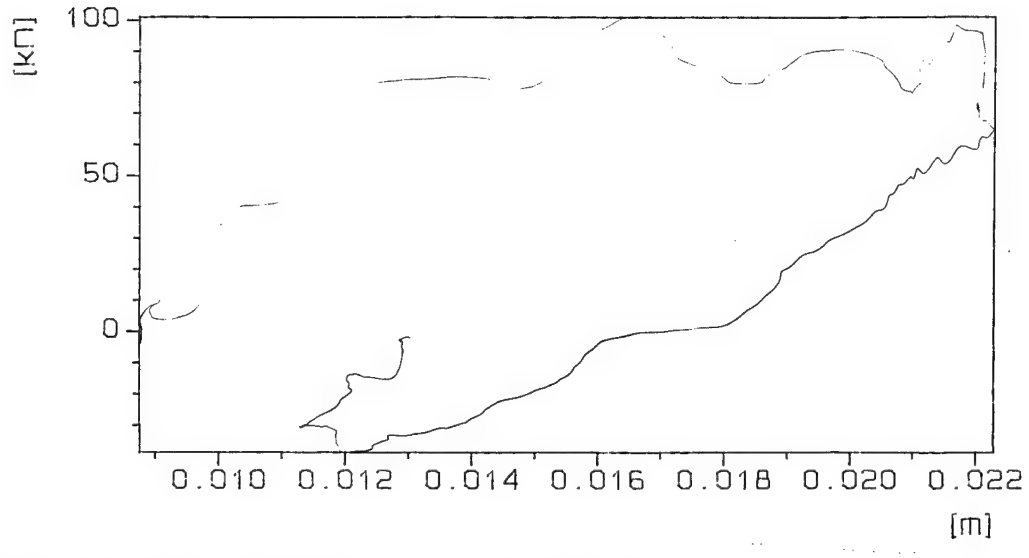

Figure 3.6c: Resistance-deformation curve of slab 2 - third test.

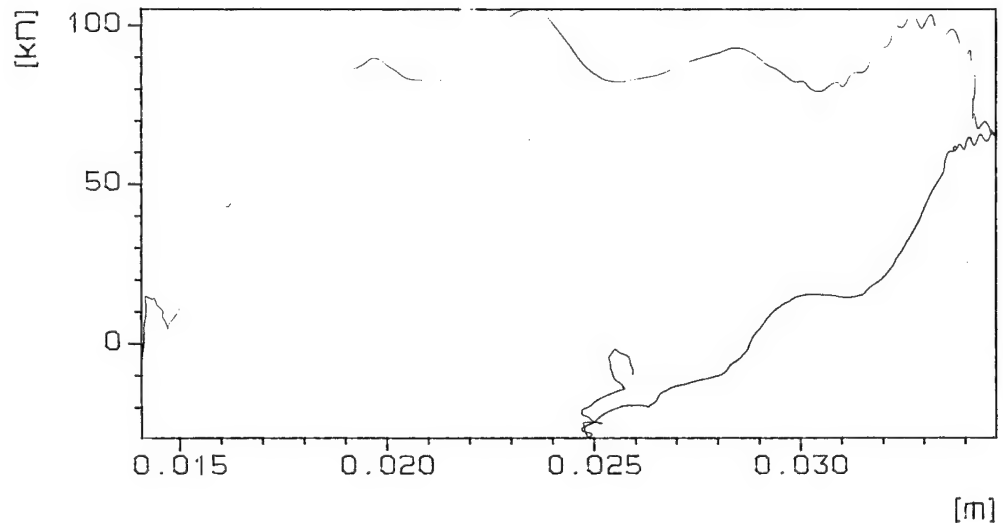

Figure 3.6d: Resistance-deformation curve of slab 2 - fourth test.

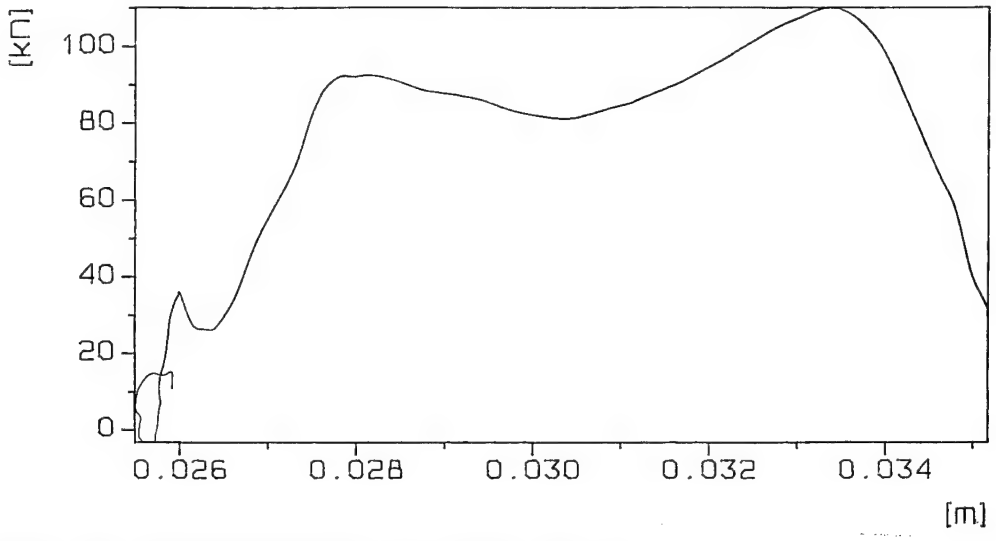

Figure 3.6e: Resistance-deformation curve of slab 2 - fifth test.

From these curves, it can be seen that the maximum resistance of the slab is about 90 kN.

- The permanent deflection after the first test is 4 mm, which corresponds with a support rotation of 0.4°.
- The permanent deflection after the second test is 7.8 mm, which corresponds with a total support rotation of 0.8°.
- The permanent deflection after the third test is 12.9 mm, which corresponds with a total support rotation of 1.3°.
- The permanent deflection after the fourth test is 24.8 mm, which corresponds with a support rotation of 2.6°.
- The deflection at failure is 35.3 mm, which corresponds with an average support rotation of 3.8°.

The energy absorbed by the slab is equal to the surface underneath the resistance-deformation curve and has been calculated to be 0.8 kJ for test 1, 0.85 kJ for test 2, 0.98 kJ for test 3, 1.55 kJ for test 4 and almost 0.8 kJ for test 5. The total energy absorbed by the slab is equal to 4.98 kJ.

3.4 Slab 3

The tests on this slab were performed on March 29th, 1996. The slab was loaded by 2 subsequent shock waves, which were each generated by 70 litres of oxygen-acetylene mixture with a mass ratio of 1 - 1. It failed after the second shock, and the failure crack was located at A3. This can be explained in the same way as the previous tests.

The global crack pattern is sketched for each one of the 2 tests in Figure 3.7. Cracks were first formed symmetrically at D2 (at the centre of the slab) and at A2

and A3. Then, asymmetry occurred and the slab failed on one of the two cracks already formed alongside the centre, by chance. Figure 3.8 shows the real crack pattern for each test.

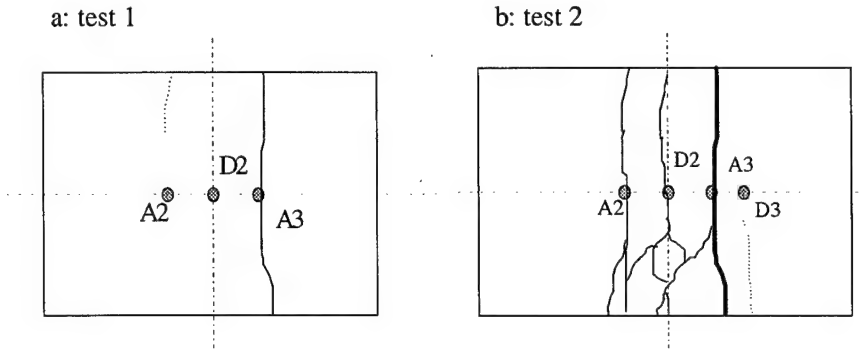

Figure 3.7: Global crack pattern in slab 3.
a: after test 1; b: after test 2.

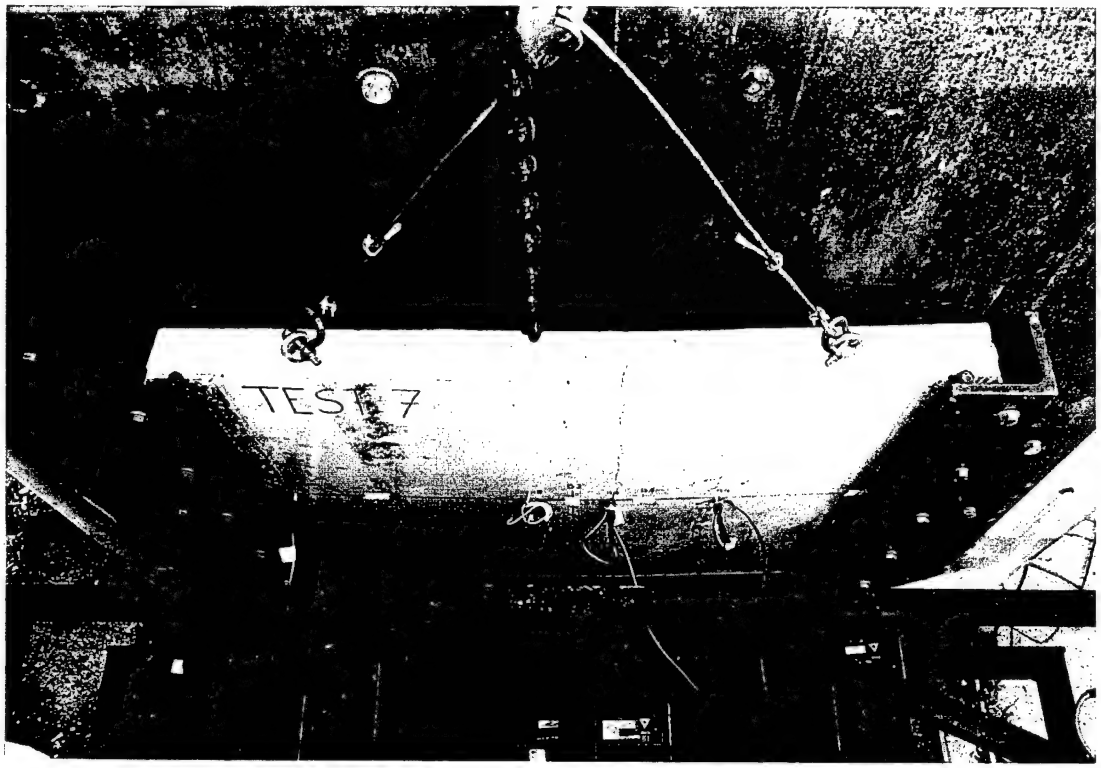

Figure 3.8a: Picture of the real crack pattern in slab 3 - test 1.

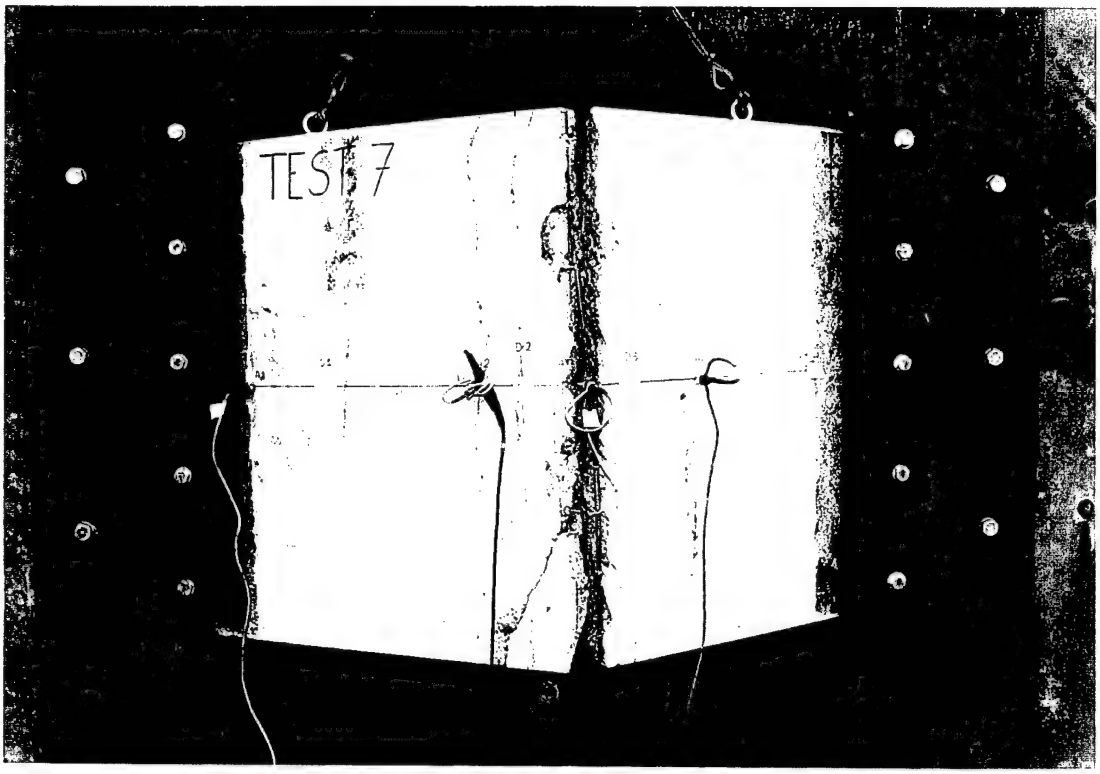

Figure 3.8b: Picture of the real crack pattern in slab 3 - test 2.

Figure 3.9 shows the resistance-deformation curve of the slab, for each test. The deformation in this curve represents the deflection at the centre of the slab for the first test, and at the failure point A3 for the second test.
From these curves, it can be seen that the maximum resistance of the slab is about 91 kN.
The permanent deflection after test 1 is 12 mm, which corresponds with a support rotation of 1.3°. The deflection at failure is 37 mm, which corresponds with an average support rotation of 3.9°.
The energy absorbed by the slab is equal to the surface underneath the resistance-deformation curve and has been calculated to be 1.35 kJ for test 1 and 1.95 kJ for test 2. The total energy absorbed by the slab is equal to 3.3 kJ.

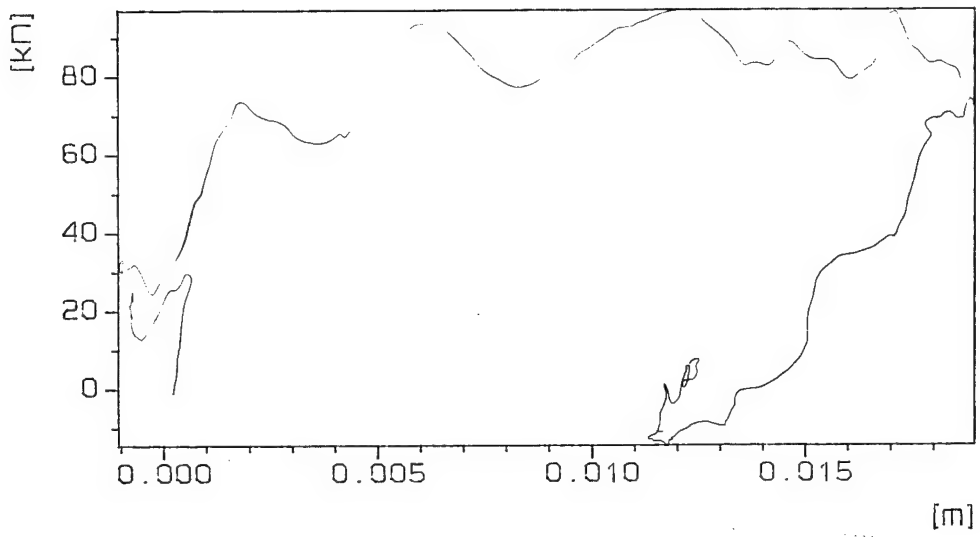

Figure 3.9a: Resistance-deformation curve of slab 3 - test 1.

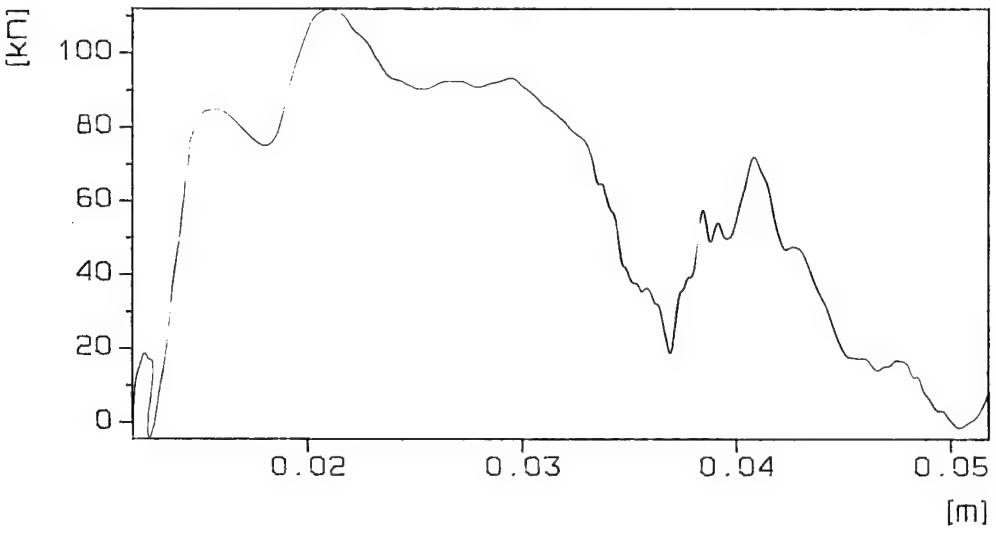

Figure 3.9b: Resistance-deformation curve of slab 3- test 2.

3.5 Slab 4

The test on this slab with stirrups was performed on April 1st, 1996. The slab was loaded by a shock wave generated by 110 litres of oxygen-acetylene mixture with a mass ratio of 1 - 1. It failed after one shock, and the failure crack was located at D2, where a transverse reinforcement bar was located.
The global crack pattern is sketched in Figure 3.10. Figure 3.11 shows the real crack pattern.

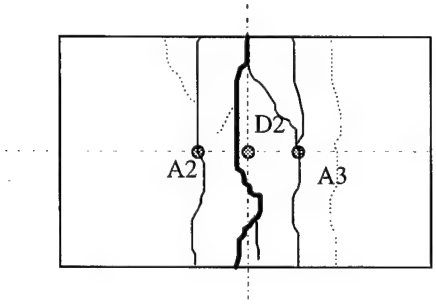

Figure 3.10: Global crack pattern in slab 4.

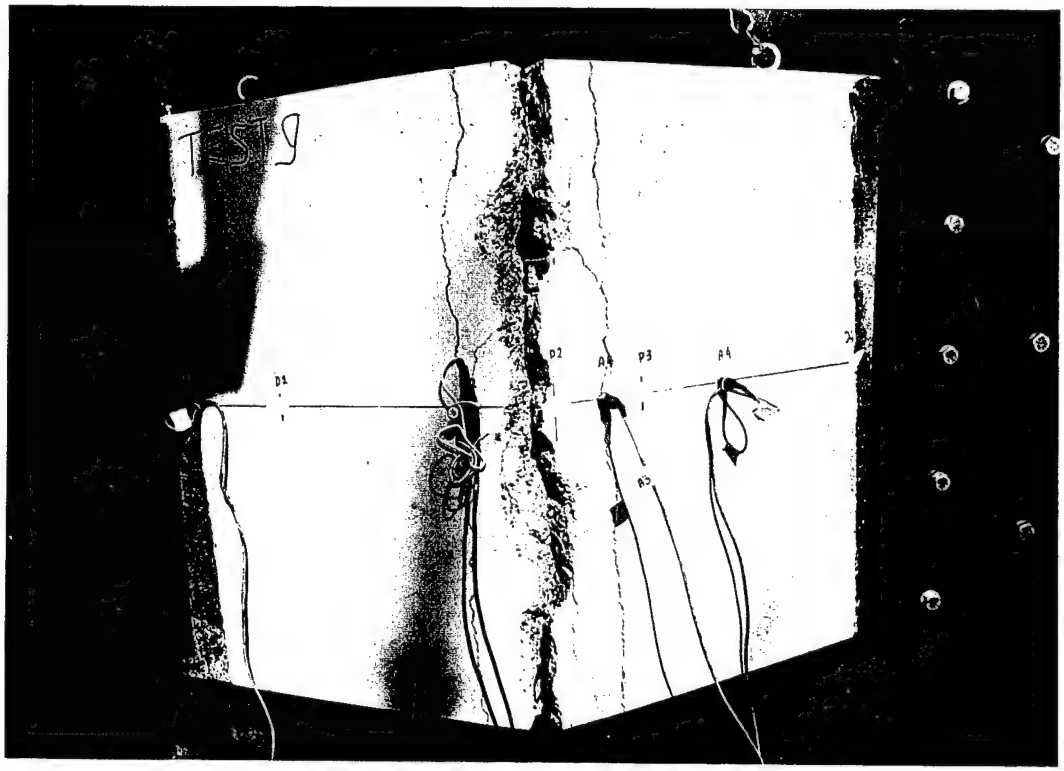

Figure 3.11: Picture of the real crack pattern in slab 4.

Figure 3.12 shows the resistance-deformation curve of the slab. The deformation in this curve represents the deflection at the centre of the slab.

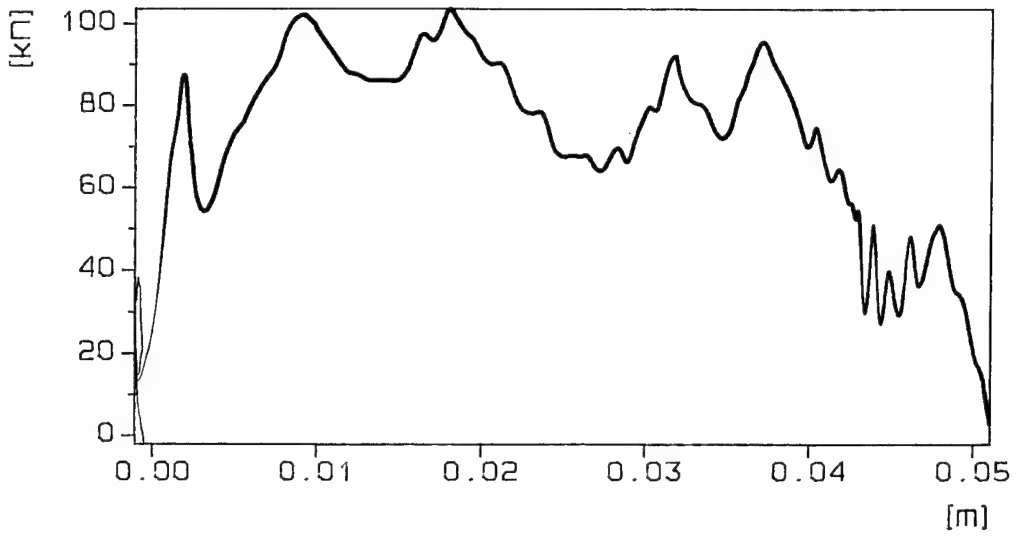

Figure 3.12: Resistance-deformation curve of slab 4.

From this curve, it can be seen that the maximum resistance of the slab is about 90 kN. The deflection at failure is 43 mm, which corresponds with a support rotation of 4.5°.
The energy absorbed by the slab is equal to the surface underneath the resistance-deformation curve and has been calculated to be 3.5 kJ.

3.6 Slab 5

The test on this slab with stirrups was performed on April 2nd, 1996. The slab was loaded by a shock wave generated by 110 litres of oxygen-acetylene mixture with a mass ratio of 1 - 1. It failed after one shock, and the failure crack was located at D2, where a transverse reinforcement bar was located.
The global crack pattern is sketched in Figure 3.13. Figure 3.14 shows the real crack pattern.

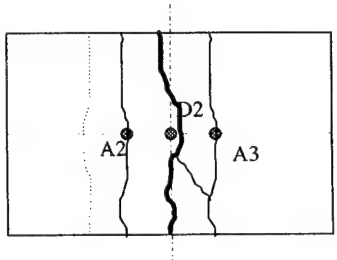

Figure 3.13: Global crack pattern in slab 5.

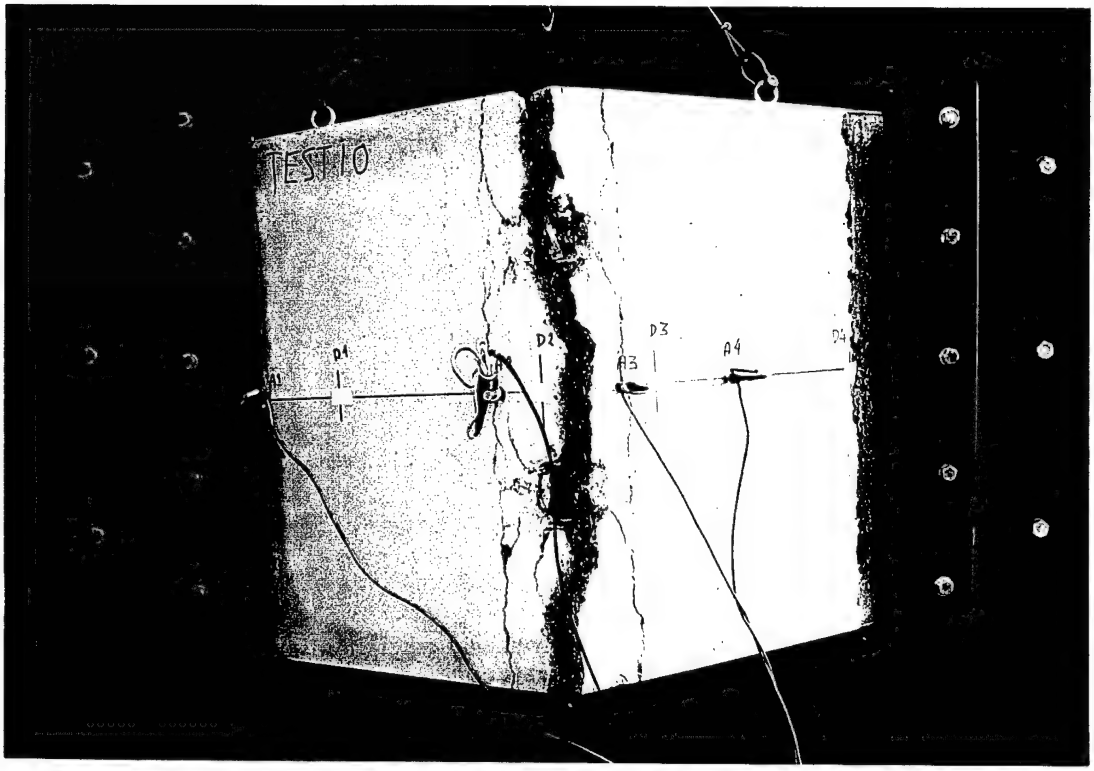

Figure 3.14: Picture of the real crack pattern in slab 5.

Figure 3.15 shows the resistance-deformation curve of the slab. The deformation in this curve represents the deflection at the centre of the slab.
From this curve, it can be seen that the maximum resistance of the slab is about 92 kN. The deflection at failure is 43 mm, which corresponds with a support rotation of 4.5°.
The energy absorbed by the slab is equal to the surface underneath the resistance-deformation curve and has been calculated to be 3.7 kJ.

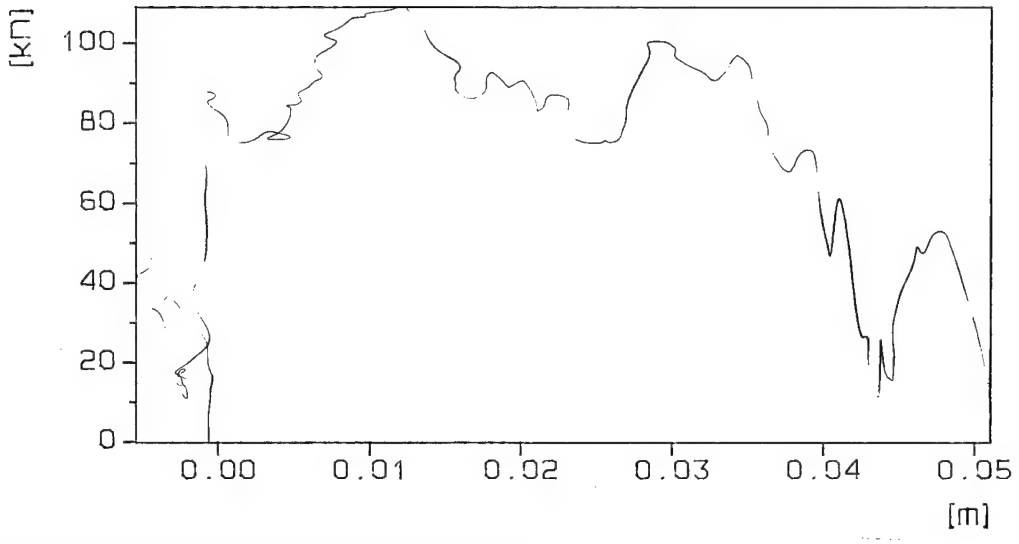

Figure 3.15: Resistance-deformation curve of slab 5.

3.7 Slab 6

The test on this slab with lacing was performed on April 2nd, 1996. The slab was loaded by a shock wave generated by 110 litres of oxygen-acetylene mixture with a mass ratio of 1 - 1. It failed after one shock, and the failure crack was located at D2, where a transverse reinforcement bar was located.
The global crack pattern is sketched in Figure 3.16. Figure 3.17 shows the real crack pattern.

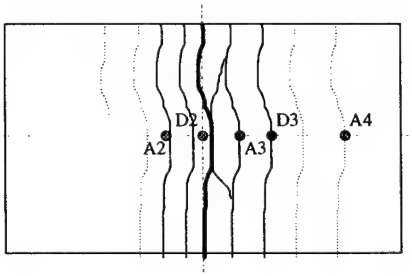

Figure 3.16: Global crack pattern in slab 6.

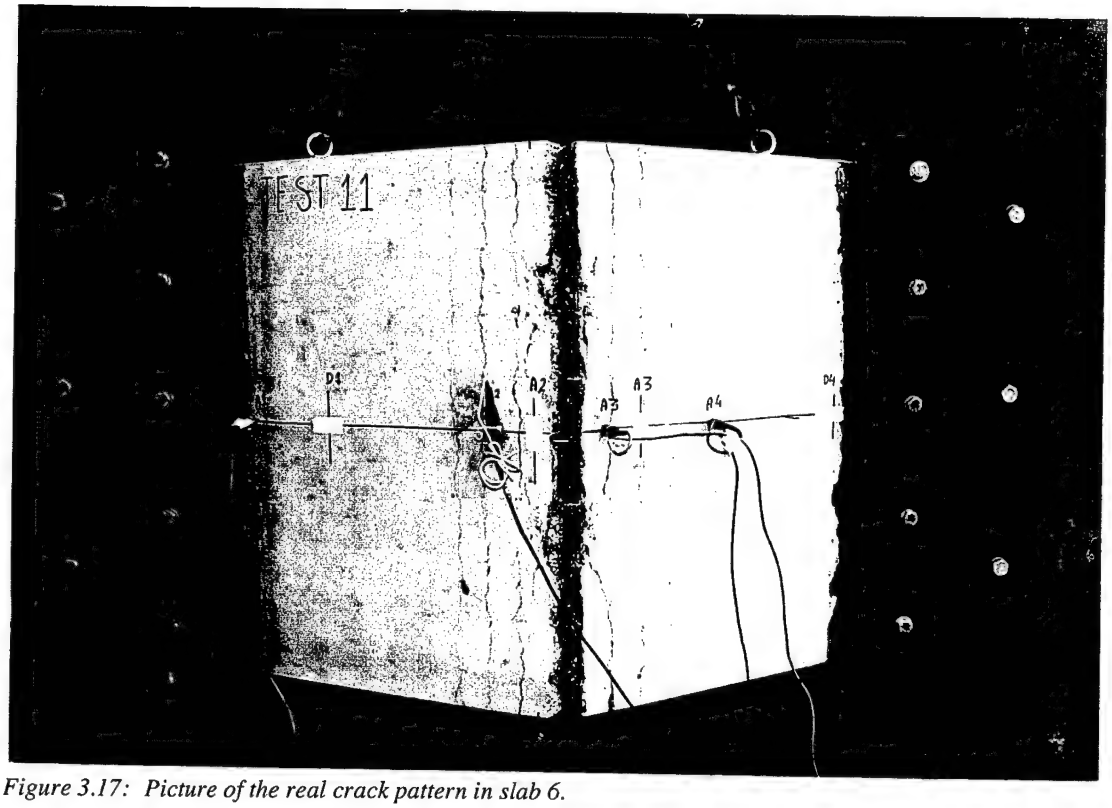

Figure 3.17: Picture of the real crack pattern in slab 6.

Figure 3.18 shows the resistance-deformation curve of the slab. The deformation in this curve represents the deflection at the centre of the slab.
This resistance-deformation curve is not that of a slab that failed but that of a slab that did not fail. Elastic springback occurs after the slab has reached its maximum deformation, which means that the load has gone and not that the resistance is lost. The acceleration measurements give the same idea. There is no sudden increase that points to a failure (see Annex D). Yet, it has been observed that the slab failed during the test. So, what has happened?
The only logical explanation that could be found for the present result is that the slab indeed did not fail due to the measured shock wave, but due to a second shock wave. This second shock wave originated from the reflected shock wave which moved back into the blast simulator to the compression chamber and was reflected there too. During this second shock data was unfortunately no longer being recorded.

From the resistance-deformation curve, it can be seen that the maximum resistance of the slab is about 93 kN. The maximum deflection is 52.2 mm, which corresponds with a support rotation of 5.4°.
The energy absorbed by the slab is equal to the surface underneath the resistance-deformation curve and has been calculated to be 4.5 kJ.

These values for the deformation and absorbed energy are underlimits for the ultimate values, which we did not obtain here.

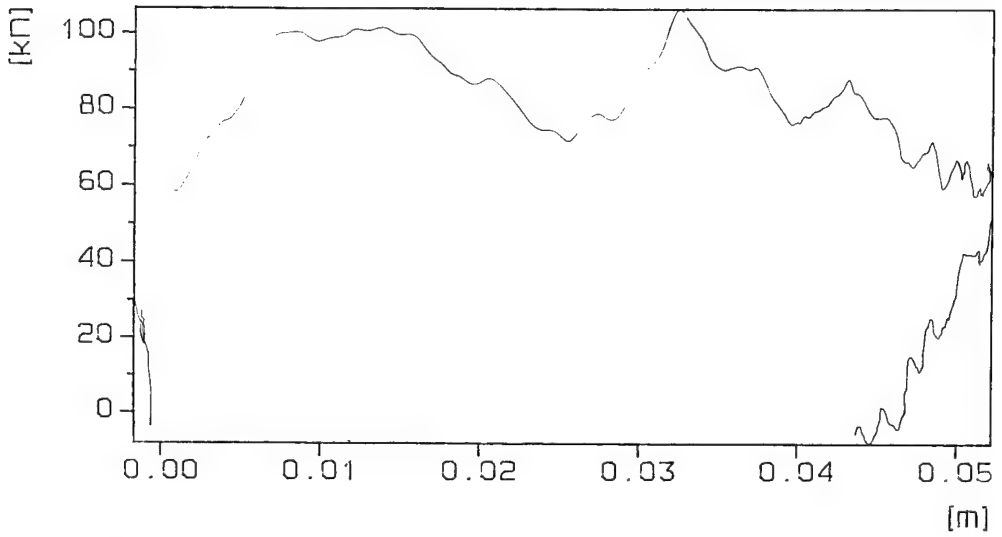

Figure 3.18: Resistance-deformation curve of slab 6.

3.8 Slab 7

The test on this slab with lacing was performed on April 2nd, 1996. The slab was loaded by a shock wave generated by 110 litres of oxygen-acetylene mixture with a mass ratio of 1 - 1. It has failed after one shock, and the failure crack was located at D2, where a transverse reinforcement bar was located.
The global crack pattern is sketched in Figure 3.19. Figure 3.20 shows the real crack pattern.

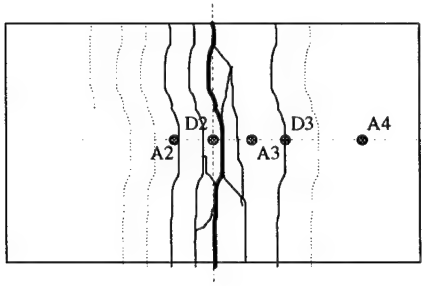

Figure 3.19: Global crack pattern in slab 7.

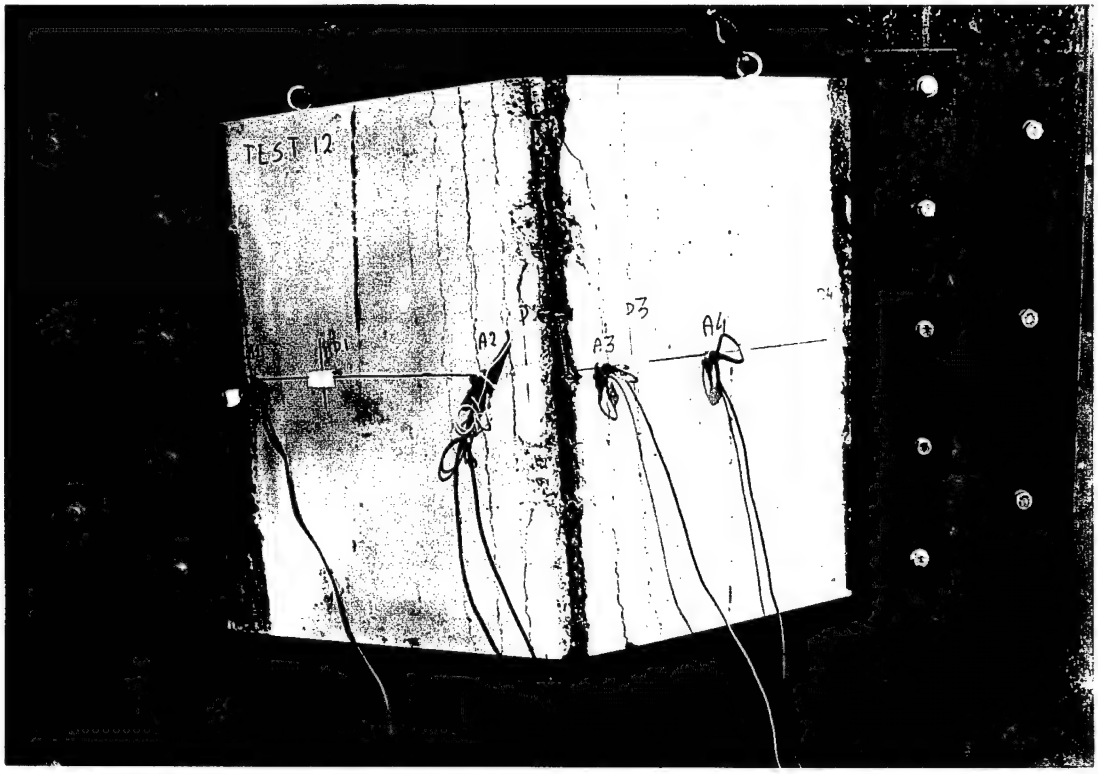

Figure 3.20: Picture of the real crack pattern in slab 7.

Figure 3.21 shows the resistance-deformation curve of the slab. The deformation in this curve represents the deflection at the centre of the slab.
Like slab 6, the resistance-deformation curve is not completely up to failure. Again, the slab did not fail due to the primary shock, but due to the secondary reflected shock, when data was no longer being recorded. Therefore, the response of the slab at failure was not registered and the acceleration signal does not show a sudden jump because of loss of resistance.

From the resistance-deformation curve, it can be seen that the maximum resistance of the slab is about 93 kN. The maximum deflection is 54.1 mm, which corresponds with a support rotation of 5.6°.
The energy absorbed by the slab is equal to the surface underneath the resistance-deformation curve and has been calculated to be 4.5 kJ.

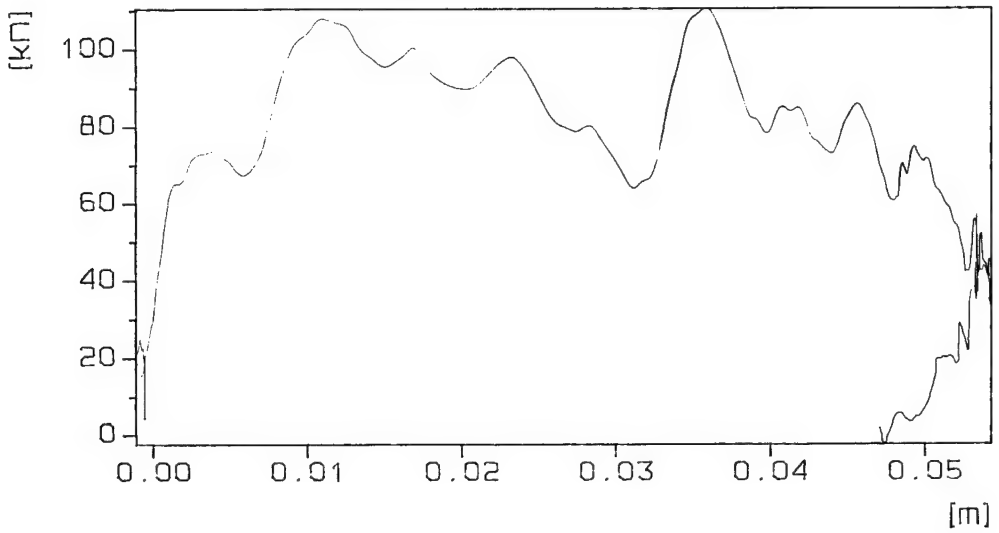

Figure 3.21: Resistance-deformation curve of slab 7.

4 Discussion of results

4.1 Introduction

In the previous chapter, the results of the tests are presented. These results will be discussed in this chapter by comparing them with each other, with the results of the previous test programme and with calculations according to TM 5-300, which are presented in Annex A.

4.2 Comparison of the present tests

To make the comparison easier, the results are summarised in Table 4.1.

Table 4.1: Summary of test results.

	Maximum resistance [kN]	Energy [kJ]	Support angle (total) [degree]
Slabs without shear reinforcement			
SLAB 1 (asymm. A3)	88	3.3	4.37 (3.69-5.04)
SLAB 2			
test 1	84	0.8	0.42
test 2	86	0.85	0.81
test 3	88	0.98	1.34
test 4	96	1.55	2.58
test 5 (asymm. A2)	95	0.8 tot=4.98	3.76 (4.34-3.18)
SLAB 3			
test 1	90	1.35	1.25
test 2 (asymm. A3)	93	1.95 tot=3.3	3.94 (3.33-4.55)
Slabs with stirrups			
SLAB 4	90	3.5	4.47
SLAB 5	92	3.7	4.47
Slabs with lacing			
SLAB 6	93	4.5*	5.42*
SLAB 7	93	4.5*	5.62*

* Is not ultimate value. Failure was not registered.

For asymmetrical failure, three angles are given in Table 4.1. The values between the brackets are the rotations at each support at failure. The other value is the average of the two support rotations. This average value is used in the following to compare the results.

The following observations can be made.

- The slabs have approximately the same resistance, about 90 kN. The type of shear reinforcement seems of no relevance for the maximum resistance. Where this result is logical for stirrups, it is not for lacing. Lacing should increase the slab's resistance. But the effective depth of these slabs (62 mm) is smaller than for slabs without tying reinforcement or with stirrups (65 mm). Apparently, the effect of the lacing on the resistance is balanced out by the decrease in effective depth.
- Slabs 4 and 5 show the same deformation capacity, and the same energy absorption capacity. The same observation can be made for slabs 6 and 7. So the results are reproduced well.
- Slabs 1 and 3 have absorbed the same amount of energy, despite the fact that we needed two shocks to make slab 3 fail. Slab 2 was brought to failure in five shocks and seemed to have absorbed much more energy. This observation cannot be explained physically. The smaller maximum deformation indicates that less energy must have been absorbed. An error must have been introduced in the calculation of the energy, an error which is due to the test method. The energy calculated for a test in which the slab does not fail is probably too high. Adding all energies of the separate tests can then cause a considerable failure, especially when the number of shocks is large: that this is the case is shown in Table 4.2, in which a rough estimate of the energy is given by multiplying the resistance of the slab with the maximum deformation. For slab 2, the result of this rough calculation, which gives an overestimate, is considerably smaller than the result from the test. It is thought that elastic energy causes the too high result, elastic energy that is only temporarily stored in the slab.

Table 4.2: Energies calculated in two different ways.

Slab no.	R max. [kN]	Deformation [mm]	Energy [kJ]	R*d [kJ]
1	88	42	3.3	3.696
2	90	35	5	3.15
3	92	37	3.29	3.404

- The deformation of slabs 4 and 5 is only slightly larger than that of slab 1.
- The ultimate deformation capacity of the slabs with lacing has not been obtained. An underestimate for the ultimate deformation capacity however is given by the maximum deformation that is measured during the test. From these values, it can be seen that slabs 6 and 7 have a larger deformation capacity than the other slabs.
- Slab 3 under two shocks failed at a little smaller deformation than slab 1 under a single shock. Slab 2 under five shocks failed at an even smaller deformation.

Three main conclusions can be made from the present programme:
First, lacing reinforcement has a distinct influence on the deformation capacity of a slab. As we have seen, slabs 6 and 7 fail at larger deformations and absorb more

energy than the other slabs. This result was expected, since lacing should improve the deformation capacity of the slab. Lacing can improve the structural integrity by its truss action; it restrains and keeps the reinforcement from buckling.
Unfortunately, we cannot quantify the increase in deformation capacity, because the slabs failed due to secondary shocks and not due to the primary shock, and the response of the slab was measured only during the first shock.
Secondly, from the comparison between slabs 4 and 5 and slab 1 it can be concluded that, at least for these slabs, stirrups do not significantly increase the deformation capacity.
Thirdly, we can conclude that it is not allowed to add the results when a slab fails in several shocks, and to compare them with those obtained when the same slab fails in one single shock. The deformation capacity is not the same.
This last conclusion does not mean that the results for slabs under multiple shocks are useless. Since the deformation capacity seems to decrease with the number of shocks, the results of multiple shock failure can safely be used for design purposes. An underestimate for the deformation capacity is obtained.

4.3 Comparison with TM 5-1300 calculation

Calculations of the slabs according to TM 5-1300 are presented in Annex A. Table 4.3 gives a direct comparison between the results.

Table 4.3: Comparison of tests and TM 5-1300.

	Slab type	R max. [kN]	Support angle [degree]
Test	3.1	90	4
TM 5-1300		91.5	2
Test	3.2	91	4.47
TM 5-1300		91.5	4
Test*	3.3	93	5.51*
TM 5-1300		91.5	12

* Slab failed because of the reflection shock wave.

For all the slabs, the maximum resistance has been predicted well with the method of TM 5-1300. This is not surprising because in previous tests the maximum resistance was also predicted well. It is well understood how a slab can build up its resistance.

With respect to the maximum deformation, the comparison of the test results with the manual gives very different results.
First, slab type 3.1, without tying reinforcement, has a considerable larger deformation capacity than TM 5-1300 permits. Compare the value of 2 degrees from TM 5-1300 with the 4 degrees found in the test. So, for these slabs, TM 5-1300 is very conservative.

The deformation of the slabs with stirrups, slab type 3.2, at failure is only a little larger than what TM 5-1300 prescribes as permissable: 4 degrees by TM 5-1300 versus 4.47 degrees experimentally found. So, for such slabs, TM 5-1300 is only slightly conservative.
For the slabs with lacing, slab type 3.3, the comparison is not fair. The value for deformation found in the test is for a situation where the slab had not yet failed. Yet, it is believed that here TM 5-1300 overestimates the capacity of the slab. It is implausible that the deformation enlarged from 5.51° to 12° or larger due to secondary shocks. It is more plausible that the deformation at which the slab failed is only a little larger than the 5.51° support rotation measured. In other tests, slabs that did not fail in a single test, did not deform a lot because of the reflection shock. This can be seen by comparing the permanent deformation after the primary shock in a test with the initial deformation in the subsequent test. These almost correspond. So, in the secondary shock waves there is only a small amount of energy present that can cause additional (plastic) deformation of the slab. This energy can only cause minor deformation.

This last conclusion is alarming. Here we have an example where TM 5-1300 seems to allow too large a deformation. Does this mean that TM 5-1300 can sometimes lead to unsafe designs? Or is there a special reason for the present result? The amount of lacing for the slab had been designed on the basis of the rules of TM 5-1300: 3 mm lacing with a spacing of 50 mm in the longitudinal direction and a spacing of 92.5 mm in the transverse direction meets the requirement of minimum area of lacing (see Annex E). Not all requirements were however satisfied. It is, for instance, also required that the lacing is uniformly distributed throughout the slab and that the maximum spacing should be limited to d_c. These conditions were not completely satisfied in the tested slab. Towards the supports, the spacing of the lacing was enlarged and exceeded the limit value. So, the amount of lacing reinforcement decreased towards the supports, but not below the required amount.
The unsatisfied requirements are not thought to be the reason for the unexpected result of the slabs with lacing. In the zone of interest, the amount of lacing was uniform and the spacing met the requirements.
There is another requirement which was not satisfied. It is required that lacing should be carried past the face of the support and securely anchored within the support. The slabs being simply supported it was not possible to anchor any reinforcement within the support. This unsatisfied requirement does not seem the reason for the unexpected result either. There was no sign of insufficient anchoring of the lacing. Anchoring past the supports is necessary when failure can occur at the supports. For failure at the centre, it is not essential.
It is thought more probable that the unexpected result has to do with the slenderness of the tested slabs. Due to the slenderness, the compression zone is very small. It is so small that the compression reinforcement initially falls within the tension zone and not in the compression zone. So, the tension zone is large and cracks are deep and wide. That means that there is no or not enough concrete that prevents the reinforcement from being pulled together when the lacing starts its

truss action. Locally, the moment of resistance then decreases very quickly and the deformation is localised. The overall deformation is then limited. This supposition is supported by the observation that the resistance decreases slowly beyond a deflection of 40 mm and by the observation on the slab after the test that the reinforcement has been pulled inwards in the slab.
Protective structures are usually not as slender as the slabs tested here. So, maybe the present result is not as alarming as it seems. Tests on thicker slabs should show this.

4.4 Comparison with previous tests

In previous tests, three parameters have been pointed out to be relevant for the deformation capacity of a concrete slab: the thickness of the slab, the reinforcement ratio and the diameter of the reinforcement. Based on the failure mode, crushing of concrete and buckling of the compression reinforcement, a combination of these factors has been found such that a single parameter defines the deformation capacity.
The maximum support rotation had appeared to be a linear function of the parameter $X = 0.85 \cdot \phi^2/(d \cdot f_{ds})$ where d is the effective depth of the slab, ϕ the reinforcement diameter and f_{ds} the dynamic design strength of the steel, or of the reduced parameter $X' = \phi^2/d$. This reduction was only possible because all slabs were reinforced with the same type of steel, i.e. f_{ds} was not a parameter in the tests. This reduction limits the validity of the empirical relationship to slabs with the same reinforcement steel. Anyhow, the validity of the empirical relationship is limited to slabs within the same category as the tested slabs, because it is only known for these slabs that they will fail in the same mode, crushing of concrete and buckling of the compression reinforcement.
The limitations for application of the empirical relationship are given next:

- no shear reinforcement;
- support length = 1.1 m;
- 70 mm < thickness < 100 mm;
- 0.35% < reinforcement ratio < 0.64%;
- reinforcement steel: FeB500;
- cube strength of concrete: 40 to 50 MPa.

Slab type 3.1 without shear reinforcement, with a support length of 1.1 m, with a thickness of 80 mm, a reinforcement ratio of 0.483%, with FeB500 as reinforcement steel and of a concrete with a cube strength of 42.5 MPa satisfies the conditions. So, it is interesting to check whether the results on this type of slab fit with the linear function.
In Table 4.4, the parameter X′ and the deformation capacity are given for all tested slabs. In Figure 4.1, each combination of X′ and ϕ_{max} are plotted.
For slab type 1.1 two values are given in Table 4.4. Two different results were namely obtained for the deformation capacity. The larger value corresponded with

a central failure, the lower with an asymmetric failure. This observation, however, did not give a satisfactory explanation for the large difference in deformation capacity. From the crack pattern, it was observed that the plastic zone was smaller for the asymmetric failure, and therefore it seems logical that the plastic zone can deform less before failure. It is, however, not understood why the plastic zone was smaller.

Uncertainties in the accuracy of the results also make it difficult to explain the differences. In the first test series (series 1.1 and 1.2), when the test method was tried out, it was not completely under control, especially not the protection of the measurement equipment. Consequently the equipment failed often and the response of the slab was measured only partly. In a later series, the problem of falling out of the equipment was overcome.

Both values for slab type 1.1 must be taken into account, because there is no indication of one of them being incorrect.

Table 4.4: Parameter X' for each slab.

Slab type	Reinforcement diameter [mm]	d [mm]	Parameter X'	Deformation capacity [degree]
1.1*	6	57	0.63	
1**				5.7
2**				3.6
1.2*	6	57	0.63	5.8
2.1*	8	83	0.77	8
2.2*	6	82	0.44	2.5
3.1.1	6	65	0.55	4.37
3.1.2	6	65	0.55	3.76
3.1.3	6	65	0.55	3.94

* Previous tests results.

** For this slab type, two different results were obtained.

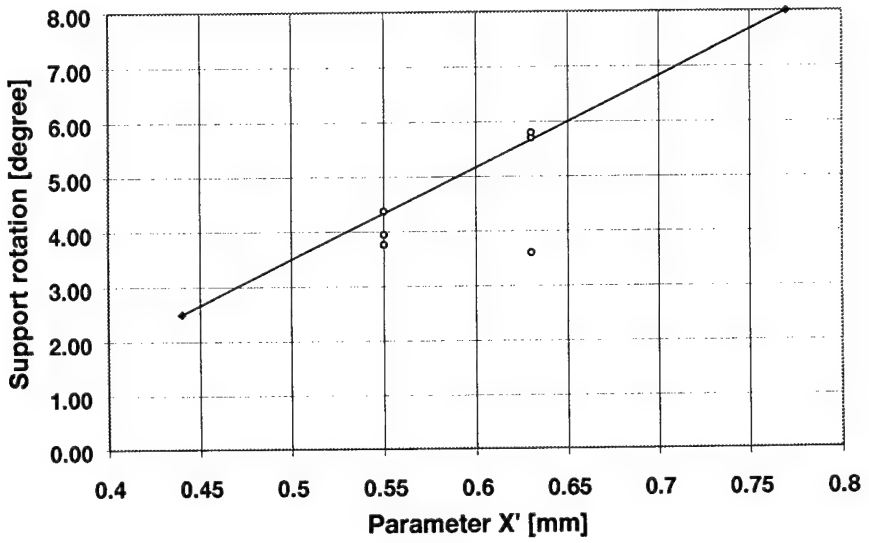

Figure 4.1: Maximum support rotation as a function of X'.

The first test result, for slab 3.1.1, gives a point located approximately on the straight line, whereas the other results, for slabs 3.1.2 and 3.1.3, do not. The results for slabs 2 and 3 do not correspond with the previous ones because they did not fail in a single shock.
Apparently, the present results fit within the previous test results. They support the validity of the empirical relationship.

5 Conclusions

Using the blast simulator at TNO-PML, blast tests were performed on simply supported reinforced concrete slabs. These slabs had the following dimensions: length of 1.2 m, support length of 1.1 m, width of 0.85 m and thickness of 80 mm. The slabs were reinforced with longitudinal reinforcement. Some of them had also shear reinforcement in the form of either stirrups or lacing. The slabs without shear reinforcement were brought to failure by a different number of shocks. The slabs with stirrups failed in one shock. The slabs with lacing failed in one trial but afterwards it appeared they had failed by the reflection shock wave.
As a result of the experiments, the resistance-deformation curves of the slabs were obtained. These curves provide much information on the behaviour of the tested slabs. They can therefore be used to increase the understanding of the behaviour of reinforced concrete slabs under a dynamic load.
Unfortunately, for the slabs with lacing, the resistance-deformation curve is not completely up to failure of the slab. The slab first failed by the reflection shock wave and, at that point in time, the response was not being measured. This means that the deformation capacity of the slabs with lacing has not been found.
The only solution, in order to prevent the same problem in future tests, is to use another recording system with more capacity, so that the response can be measured during a longer period.

Analysis and comparison of the present and previous tests led to the following observations and conclusions.

- The result for the slabs without shear reinforcement fits within the previous results. So, this result supports the empirical relationship with parameter X, composed of the influence factors of the slab.
- The deformation capacity of the slabs with stirrups was only slightly larger than that of the slabs without stirrups.
- Slabs seem to have a lower deformation capacity under multiple shocks. So, the deformation at which a slab fails under multiple shocks is an underestimate for the dynamic deformation capacity under a single shock.
- Lacing reinforcement has a distinct influence on the deformation capacity of the slabs.

A comparison of the test results with a calculation according to the design rules of TM 5-1300 showed that these rules are not always conservative. Even the opposite has been observed. For the slabs without shear reinforcement, TM 5-1300 prescribes too low a value for the capacity (2 versus 4 degrees). For the slabs with stirrups, the deformation capacity was only slightly underpredicted by TM 5-1300 (4 versus 4.5 degrees). The slabs with lacing however failed at a much smaller support rotation (approximately 6 degrees) than the 12 degrees given by TM 5-1300. These results point out that TM 5-1300 should be used with care.

The most probable explanation for the small support rotation of the laced slabs is that, due to the slenderness of the slab, the truss action of the lacing localises the deformation too much. Due to deep cracks and the truss action, locally the reinforcement is pulled inwards and the moment capacity is reduced. So deformation is limited to this location.
This assumption should be investigated with tests on thicker slabs; the doubts on the rules of TM 5-1300 might be then taken away.

For the next phase of the project, the following proposition is therefore given: perform tests on thicker slabs to check the hypothesis given above. Slabs with all three types of reinforcement should be performed. Slabs without shear reinforcement are needed as reference and either to extend the validity of the empirical relationship or to demarcate its validity (change of failure mechanism). Slabs with stirrups should be tested because it is expected that they will have a more pronounced effect in thicker slabs. Slabs with lacing should be tested to check whether the above hypothesis about the slenderness of the slab and the truss action of lacing is correct.

6 References

[1] Doormaal, J.C.A.M. van,
Dynamic deformation capacity of reinforced concrete. Phase 2- Test method,
TNO Prins Maurits Laboratorium, PML 1995-A24, Rijswijk, May 1995.

[2] Doormaal, J.C.A.M. van,
Dynamic deformation capacity of reinforced concrete. Phase 3- Experiments on simply supported slabs,
TNO Prins Maurits Laboratorium, PML 1995-A82, Rijswijk, December 1995.

[3] Doormaal, J.C.A.M. van,
Dynamische vervormingscapaciteit van gewapend beton. Fase 1: Literatuuronderzoek,
TNO Prins Maurits Laboratorium, PML 1993-24, Rijswijk, 1993.

[4] TM 5-1300,
Departments of the American Army, the Navy and the Air Force, Structures to resist the effect of accidental explosives,
Washington DC, 19 November 1991.

7 Authentication

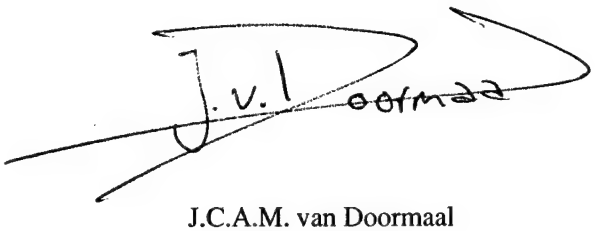

Dr. J. Weerheijm
Group leader

J.C.A.M. van Doormaal
Author

Annex A Calculations according to TM 5-1300

Calculations with TM 5-1300 are carried out for two reasons. The first reason is to obtain an idea of the response of the slab and of the shock waves needed in the tests. Secondly, the calculations are used to compare the test results with the design rules of TM 5-1300.

In the calculations, the strength characteristics of the reinforcement, as given by the manufacturer, are increased by 10%, as is advised by TM 5-1300 itself. Furthermore, the strength characteristics of the steel as well as the concrete are multiplied with the so-called dynamic increase factors, which are given in Table 4.1.

For the calculation of the ultimate moment in a cross-section, the formula for concrete with both tensile and compression reinforcement has been used, because in the previous test series it had appeared that the resistance of the slabs was predicted best with this equation. This formula is given by

$$M_u = Wpdf_{ds}(d - \frac{a}{2}) + Wpdf_{ds}(d - d' - \frac{a}{2})$$

with d' = distance between compression and tension steel = d - c - $\phi/2$ $d - c - \frac{\phi}{2}$.

The results of the calculations are given next.

A.1 Slabs without tying reinforcement

Dimensions of slabs		
Length L	1.2	m
Support length L_s	1.1	m
Width W	0.85	m
Height H	0.08	m
Mass M_{tot}	213.56	kg
Mass of angle sections M_{as}	12.6	kg
Reinforcement		
Symmetric		
Diameter	6	mm
In-between distance b	92.5	mm
Concrete cover c	12	mm
Number of rods n	9	
Ratio	0.483	%
Properties of concrete		
Cube strength f_c	48.6	MPa
Young' s modulus E_c	29.6	GPa
Poisson's ratio	0.2	

Properties of steel

Yield strength f_y		550	MPa
Ultimate strength f_u	>=	638	MPa
Young's modulus E_s		210	GPa

Table 4.1 of TM 5-1300

f_{dy}/f_y=	1.17
f_{du}/f_u=	1.05
f'_{dc}/f'_c=	1.19

Dynamic strength properties

f_{dy}=	643.5	MPa
f_{du}=	669.9	MPa
f'_{dc}=	57.834	MPa

Dynamic design stress

f_{ds}=	650.1	MPa

Other useful values

Effective depth of the slab	d=	65	mm
Distance between compression and tensile steel	d'=	50	mm
Area of tension reinforcement	A_s=	28.27	mm^2
Amount of reinforcement	p=	0.0046058	
a (for the maximum moment)	a=	3.96	mm
Maximum moment M_u	M_u=	12579.47	Nm
$m= E_s/E_c$	m=	7.09	
Figure 4.12 of TM 5-1300 for F	F=	0.0255	
I_g (for the average moment of inertia)	I_g=	3.63E+07	mm^4
I_c (for the average moment of inertia)	I_c=	5.95E+06	mm^4
Average moment of inertia I_a	I_a=	2.11E+07	mm^4
Mass of the element between its supports	M=	184.2133	kg
Maximum resistance of simply supported slab	R_u=	91487.07	N
Stiffness	K_e=	3.61E+07	N/m
Maximum elastic strain	X_e=	2.54E+00	mm

Table 3.12 of TM 5-1300 for K_{LM}

Elastic	0.78
Plastic	0.66
Average	0.72

Equivalent mass	M_e=	132.63	kg
Natural period	T_n=	12.05	ms

Is failure due to shear?

Dynamic increase factor for the strength properties of concrete under shear loading is equal to 1.1

Dynamic cube strength	53.46	MPa
Shear capacity	1.23	MPa
Maximum shear stress	0.73	MPa

If maximum shear stress<= Shear capacity, then failure is not due to shear, otherwise it is.

Shock waves necessary to bring the slab to failure

Ultimate support rotation of 4.4 deg = 0.0767945 (rad)

X_m= 42.32 mm

X_m/X_e= 16.68

$R_u/(P_{peak}*0.8)$	P_{peak} (kPa)	T/T_n	T
0.1	1143.59	0.19	2.29
0.2	571.79	0.4	4.82
0.3	381.20	0.65	7.83
0.4	285.90	0.925	11.15
0.5	228.72	1.3	15.67
0.6	190.60	1.8	21.69
0.7	163.37	2.7	32.54
0.8	142.95	4.6	55.44
0.9	127.07	9.5	114.49

Pressure and period for a 2 shock(s) failure

Support rotation of 2.20 deg = 0.0383972 (rad)

X_m= 21.13 mm

X_m/X_e= 8.33

$R_u/(P_{peak}*0.8)$	P_{peak} (kPa)	T/T_n	T
0.1	1143.59	0.3	3.62
0.2	571.79	0.28	3.37
0.3	381.20	0.44	5.30
0.4	285.90	0.625	7.53
0.5	228.72	0.85	10.24
0.6	190.60	1.15	13.86
0.7	163.37	1.7	20.49
0.8	142.95	2.6	31.33
0.9	127.07	4.8	57.85

Pressure and period for a 3 shock(s) failure

Support rotation of 1.47 deg = 0.0255982 (rad)

X_m= 14.08 mm

X_m/X_e= 5.55

$R_u/(P_{peak}*0.8)$	P_{peak} (kPa)	T/T_n	T
0.1	1143.59	0.11	1.33
0.2	571.79	0.22	2.65
0.3	381.20	0.34	4.10
0.4	285.90	0.48	5.78
0.5	228.72	0.65	7.83
0.6	190.60	0.85	10.24
0.7	163.37	1.2	14.46
0.8	142.95	1.7	20.49
0.9	127.07	2.9	34.95

Support rotation for combinations of pressure-period which can be generated in the blast simulator of TNO-PML

P_{peak} (kPa)	160	150	65	32
T (ms)	65	55	40	25
T/T_n	5.39	4.56	3.32	2.07
R_u/P	0.71	0.76	1.76	3.57
X_m/X_e	>=100	80	1.5	0.5
X_m (mm)	#VALUE!	203.00	3.81	1.27
angle (deg)	#VALUE!	20.26	0.40	0.13
number of shocks	/	1	12	34

Method using Energy

Energy used in one shock (assume) 4 kJ

Energy necessary to bring the slab to failure

Value $(X_m-X_e)*R_u + 0.5*R_u*X_e$

Support rotation of	4.4	2.20	1.47	deg
Energy	3.76	1.82	1.17	kJ
Total energy	3.76	3.63	3.52	kJ
Number of shocks necessary	1.00	1.00	1.00	

A.2 Slabs with stirrups

Dimensions of slabs		
Length L	1.2	m
Support length L_s	1.1	m
Width W	0.85	m
Height H	0.08	m
Mass M_{tot}	213.56	kg
Mass of angle sections M_{as}	12.6	kg

Reinforcement		
Symmetric		
Diameter	6	mm
In-between distance b	92.5	mm
Concrete cover c	12	mm
Number of rods n	9	
Ratio	0.483	%

Properties of concrete		
Cube strength f_c	48.6	MPa
Young' s modulus E_c	29.6	GPa
Poisson's ratio	0.2	

Properties of steel		
Yield strength f_y	550	MPa
Ultimate strength f_u >=	638	MPa
Young's modulus E_s	210	GPa

Table 4.1 of TM 5-1300

f_{dy}/f_y=	1.17
f_{du}/f_u=	1.05
f'_{dc}/f'_c=	1.19

Dynamic strength properties		
f_{dy}=	643.5	MPa
f_{du}=	669.9	MPa
f'_{dc}=	57.834	MPa
Dynamic design stress		
f_{ds}=	650.1	MPa

Other useful values

Effective depth of the slab	d=	65	mm
Distance between compression and tensile steel	d'=	50	mm
Area of tension reinforcement	A_s=	28.27	mm^2
Amount of reinforcement	p=	0.0046058	
a (for the maximum moment)	a=	3.96	mm
Maximum moment M_u	M_u=	12579.47	Nm
m= E_s/E_c	m=	7.09	
Figure 4.12 of TM 5-1300 for F	F=	0.0255	
I_g (for the average moment of inertia)	I_g=	3.63E+07	mm^4
I_c (for the average moment of inertia)	I_c=	5.95E+06	mm^4
Average moment of inertia I_a	I_a=	2.11E+07	mm^4
Mass of the element between its supports	M=	184.21333	kg
Maximum resistance of simply supported slab	R_u=	91487.074	N
Stiffness	K_e=	3.61E+07	N/m
Maximum elastic strain	X_e=	2.54E+00	mm

Table 3.12 of TM 5-1300 for K_{LM}

Elastic	0.78
Plastic	0.66
Average	0.72

Equivalent mass	M_e=	132.63	kg
Natural period	T_n=	12.05	ms

Is failure due to shear?

Dynamic increase factor for the strength properties of concrete under shear loading is equal to 1.1

Dynamic cube strength	53.46	MPa
Shear capacity	1.23	MPa
Maximum shear stress	0.73	MPa

If maximum shear stress<= Shear capacity then failure is not due to shear, otherwise it is.

Shock waves necessary to bring the slab to failure

Ultimate support rotation of 4 deg = 0.0698132 (rad)

X_m= 38.46 mm

X_m/X_e= 15.16

$R_u/(P_{peak}*0.8)$	P_{peak} (kPa)	T/T_n	T
0.1	1143.59	0.18	2.17
0.2	571.79	0.28	3.37
0.3	381.20	0.6	7.23
0.4	285.90	0.875	10.54
0.5	228.72	1.25	15.06
0.6	190.60	1.7	20.49
0.7	163.37	2.5	30.13
0.8	142.95	4.3	51.82
0.9	127.07	7.5	90.38

Shock waves necessary to bring the slab to failure

Ultimate support rotation of 5 deg = 0.0872665 (rad)

X_m= 48.12 mm

X_m/X_e= 18.96

$R_u/(P_{peak}*0.8)$	P_{peak} (kPa)	T/T_n	T
0.1	1143.59	0.2	2.41
0.2	571.79	0.43	5.18
0.3	381.20	0.6	7.23
0.4	285.90	1	12.05
0.5	228.72	1.43	17.23
0.6	190.60	1.95	23.50
0.7	163.37	3	36.15
0.8	142.95	5.1	61.46
0.9	127.07	10.5	126.54

Ultimate support rotation of 6 deg = 0.1047198 (rad)

X_m= 57.81 mm

X_m/X_e= 22.78

$R_u/(P_{peak}*0.8)$	P_{peak} (kPa)	T/T_n	T
0.1	1143.59	0.22	2.65
0.2	571.79	0.47	5.66
0.3	381.20	0.67	8.07
0.4	285.90	1.1	13.26
0.5	228.72	1.7	20.49
0.6	190.60	2.2	26.51
0.7	163.37	3.4	40.97
0.8	142.95	5.8	69.90
0.9	127.07	12.7	153.05

Ultimate support rotation of 7 deg = 0.122173 (rad)

X_m= 67.53 mm

X_m/X_e= 26.61

$R_u/(P_{peak}*0.8)$	P_{peak} (kPa)	T/T_n	T
0.1	1143.59	0.24	2.89
0.2	571.79	0.5	6.03
0.3	381.20	0.8	9.64
0.4	285.90	1.2	14.46
0.5	228.72	1.7	20.49
0.6	190.60	2.4	28.92
0.7	163.37	3.6	43.38
0.8	142.95	6.3	75.92
0.9	127.07	14	168.72

Maximum deformation with the blast simulator capacities

Maximum pressure		P_{peak}=	160	kPa
Maximum period		T=	65	ms
Figure 3-54 of TM 5-1300 gives				
	with	T/T_n=	5.39	
	and	R_u/P=	0.71	
	then	X_m/X_e=	>=100	
	Other choice	T=	50	ms
	then	T/T_n=	4.15	
	and	X_m/X_e=	34	
	So	X_m=	86.27	mm
Support rotation			8.91	deg
Number of shocks to bring the slab to failure			1	

Method using Energy

Energy used in one shock 4 kJ

Energy necessary to bring the slab to failure

Value $(X_m-X_e)*R_u + 0.5*R_u*X_e$

Support rotation of	5	6	7	deg
Energy	4.29	5.06	6.06	kJ
Number of shocks necessary	2.00	2.00	2.00	

A.3 Slabs with lacing

Dimensions of slabs

Length L	1.2	m
Support length L_s	1.1	m
Width W	0.85	m
Height H	0.08	m
Mass M_{tot}	213.56	kg
Mass of angle sections M_{as}	12.6	kg

Reinforcement

Symmetric		
Diameter	6	mm
In-between distance b	92.5	mm
Concrete cover c	15	mm
Number of rods n	9	
Ratio	0.483	%

Properties of concrete

Cube strength f_c	48.6	MPa
Young' s modulus E_c	29.6	GPa
Poisson's ratio	0.2	

Properties of steel

Yield strength f_y		550	MPa
Ultimate strength f_u	>=	638	MPa
Young's modulus E_s		210	GPa

Table 4.1 of TM 5-1300

f_{dy}/f_y=	1.17
f_{du}/f_u=	1.05
f'_{dc}/f'_c=	1.19

Dynamic strength properties

f_{dy}=	643.5	MPa
f_{du}=	669.9	MPa
f'_{dc}=	57.834	MPa

Dynamic design stress

f_{ds}=	650.1	MPa

Other useful values

Effective depth of the slab	d=	62	mm
Distance between compression and tensile steel	d'=	44	mm
Area of tension reinforcement	A_s=	28.27	mm^2
Amount of reinforcement	p=	0.0048286	
a (for the maximum moment)	a=	3.96	mm
Maximum moment M_u	M_u=	12579.47	Nm
$m= E_s/E_c$	m=	7.09	
Figure 4.12 of TM 5-1300 for F	F=	0.0257	
I_g (for the average moment of inertia)	I_g=	3.63E+07	mm^4
I_c (for the average moment of inertia)	I_c=	5.21E+06	mm^4
Average moment of inertia I_a	I_a=	2.07E+07	mm^4
Mass of the element between its supports	M=	184.21333	kg
Maximum resistance of simply supported slab	R_u=	91487.074	N
Stiffness	K_e=	3.54E+07	N/m
Maximum elastic strain	X_e=	2.58E+00	mm

Table 3.12 of TM 5-1300 for K_{LM}

Elastic	0.78
Plastic	0.66
Average	0.72

Equivalent mass	M_e=	132.63	kg
Natural period	T_n=	12.16	ms

Slabs failure will not be due to shear

Shock waves necessary to bring the slab to failure

Ultimate support rotation of 12 deg = 0.2094395 (rad)

X_m= 116.91 mm

X_m/X_e= 45.26

$R_u/(P_{peak}*0.8)$	P_{peak} (kPa)	T/T_n	T
0.1	1143.59	0.32	3.89
0.2	571.79	0.66	8.03
0.3	381.20	1.1	13.38
0.4	285.90	1.6	19.45
0.5	228.72	2.3	27.97
0.6	190.60	3.3	40.13
0.7	163.37	5	60.80
0.8	142.95	9	109.43

Maximum deformation with the blast simulator capacities

Maximum pressure P_{peak}= 160 kPa

Maximum period T= 65 ms

Figure 3-54 of TM 5-1300 gives

with T/T_n= 5.35

and R_u/P= 0.71

then X_m/X_e= 48

So X_m= 123.99 mm

Support rotation 12.70 deg

Number of shocks to bring the slab to failure 1

Other choice T= 40 ms

then T/T_n= 3.29

and X_m/X_e= 22.5

So X_m= 58.12 mm

Support rotation 6.03 deg

Number of shocks to bring the slab to failure 2

Method using Energy

Energy used in one shock 4 kJ

Energy necessary to bring the slab to failure

Value $(X_m-X_e)*R_u + 0.5*R_u*X_e$ = 10.58 kJ

Number of shocks necessary to bring the slab to failure 3

Annex B Concrete composition

The concrete mix was made in accordance with the VBT 1986 (NEN 5950). Furnace cement and river sand were used to make the concrete mix. A gradation of the aggregates around line B8 (maximum aggregate size of 8 mm) was realised with common concrete sand, an addition of 4 mm aggregates and of aggregates smaller than 0.25 mm. A superplastificator (1% m/m Betomix 450) was added in order to obtain the desired concrete quality.

Table B.1: Casting data of concrete.

Casting date		22-02-1996	
setting measure NEN 5956	[mm]	27	
shaking measure NEN 5957	[mm]	340	
vol. mass NEN 5959	[kg/m^3]	2208	2238
air content NEN 5962	[%(V/V)]	6.5	5.4
cement content at wcf 0.55	[kg/m^3]	311	315
slab numbers		1 t/m 3	4 t/m 7

The slabs and the specimens for the material tests were densified and after-cared as follows:

- the cement was densified with a vibrating needle per reinforcement mesh;
- the slab was smoothed using a vibrating beam and finished with a hand skimmer;
- the slabs were covered with plastic foil for four days, and then exposed to the air.

The material tests gave the mechanical properties as presented in Table B.2.

Table B.2: Mechanical properties of concrete.

slab numbers	age	cube strength NEN 5968 [N/mm^2]	splitting tensile strength NEN 5969 [N/mm^2]	E-modulus [N/mm^2]
1 t/m 3	28	40.0	3.20	26100
4 t/m 7		36.3	2.84	27100
1 t/m 3	28+7	42.5	-	-
4 t/m 7		40.3	-	-
1 t/m 3	28+12	38.6	-	-
4 t/m 7		39.2	-	-
1 t/m 3	28+13	38.8	3.75	-
4 t/m 7		38.8	3.55	-

Annex C Manipulation of measured signals

C.1 Theory for centre failure

We obtained ten signals:

- the side-on pressure at 1.5 m in front of the slab;
- the pressure load on the slab;
- four displacements at locations D1, D2, D3, and D4;
- four accelerations at locations A1, A2, A3, and A4.

These signals are used to obtain the resistance-deformation curve as follows:
it was assumed that the bending deformation of the slab can be described using the theoretically used elastic and plastic shape functions, given by

$$\phi_{el}(x) = \frac{16}{5}\left(\frac{x}{L_s}\right)^4 - \frac{24}{5}\left(\frac{x}{L_s}\right)^2 + 1$$
$$\phi_{pl}(x) = 1 - \left|\frac{2x}{L_s}\right| \qquad \text{(C.1)}$$

In the previous tests, it was observed that with these shape functions the deformation of the slabs can be described well.
Together with the rigid motion, for which the shape function $\phi(x)=1$ is valid, the acceleration and the displacement can be separated into three parts, a rigid motion, an elastic bending motion and a plastic bending motion. Mathematically this is described by

$$d(x) = d_r + \phi_{el}(x)\cdot d_{el}(0) + \phi_{pl}(x)\cdot d_{pl}(0) \qquad \text{(C.2)}$$

or

$$a(x) = a_r + \phi_{el}(x)\cdot a_{el}(0) + \phi_{pl}(x)\cdot a_{pl}(0) \qquad \text{(C.3)}$$

Each measured displacement or acceleration can be split up like this, which results in a set of four equations with three unknown parameters, d_r, $d_{el}(0)$ and $d_{pl}(0)$ or a_r, $a_{el}(0)$ and $a_{pl}(0)$. The displacements and accelerations are known in four points:

D1	x = -0.35	A1	x = -0.5
D2	x = 0	A2	x = -0.075
D3	x = 0.12	A3	x = 0.075
D4	x = 0.5	A4	x = 0.25

The set of equations for the displacement measurements is given by

$$\begin{bmatrix} d(-0.035) \\ d(0) \\ d(0.12) \\ d(0.5) \end{bmatrix} = D \begin{bmatrix} d_r \\ d_{el}(0) \\ d_{pl}(0) \end{bmatrix} \tag{C.4}$$

with D a 4*3 matrix defined by

$$D = \begin{bmatrix} 1 & \phi_{el}(-0.35) & \phi_{pl}(-0.35) \\ 1 & \phi_{el}(0) & \phi_{pl}(0) \\ 1 & \phi_{el}(0.12) & \phi_{pl}(0.12) \\ 1 & \phi_{el}(0.5) & \phi_{pl}(0.5) \end{bmatrix} \tag{C.5}$$

The set of equations for the acceleration measurements is given by

$$\begin{bmatrix} a(-0.5) \\ a(-0.075) \\ a(0.075) \\ a(0.25) \end{bmatrix} = A \begin{bmatrix} a_r \\ a_{el}(0) \\ a_{pl}(0) \end{bmatrix} \tag{C.6}$$

with A a 4*3 matrix defined by

$$A = \begin{bmatrix} 1 & \phi_{el}(-0.5) & \phi_{pl}(-0.5) \\ 1 & \phi_{el}(-0.075) & \phi_{pl}(-0.075) \\ 1 & \phi_{el}(0.075) & \phi_{pl}(0.075) \\ 1 & \phi_{el}(0.25) & \phi_{pl}(0.25) \end{bmatrix} \tag{C.7}$$

If we use the theoretical shape functions (C.1), we can calculate A and D:

$$D = \begin{bmatrix} 1 & 0.547 & 0.364 \\ 1 & 1 & 1 \\ 1 & 0.943 & 0.782 \\ 1 & 0.145 & 0.0909 \end{bmatrix} \qquad A = \begin{bmatrix} 1 & 0.145 & 0.0909 \\ 1 & 0.977 & 0.8636 \\ 1 & 0.977 & 0.8636 \\ 1 & 0.761 & 0.545 \end{bmatrix}$$

Using the least square method the inverse has been calculated. For the displacement this inverse is given by

$$\begin{bmatrix} d_r \\ d_{el}(0) \\ d_{pl}(0) \end{bmatrix} = \begin{bmatrix} 0.029 & 0.219 & -0.431 & 1.183 \\ 3.434 & -3.607 & 3.388 & -3.215 \\ -3.651 & 4.305 & -2.773 & 2.119 \end{bmatrix} \begin{bmatrix} d(-0.035) \\ d(0) \\ d(0.12) \\ d(0.5) \end{bmatrix} \tag{C.8}$$

and for the acceleration by

$$\begin{bmatrix} a_r \\ a_{el}(0) \\ a_{pl}(0) \end{bmatrix} = \begin{bmatrix} 1.266 & 0.041 & -0.041 & -0.348 \\ -3.027 & -1.887 & -1.887 & 6.802 \\ 1.904 & 2.560 & 2.560 & -7.024 \end{bmatrix} \begin{bmatrix} a(-0.5) \\ a(-0.075) \\ a(0.075) \\ a(0.25) \end{bmatrix} \quad \text{(C.9)}$$

The inertia forces $F_{inertia}$ are calculated by multiplying the different acceleration contributions with the effective masses, which are respectively equal to 248.5 kg for the rigid motion, 0.78·216.2 = 168.6 kg for the elastic motion and 0.66·216.2 = 142.7 kg for the plastic motion.

$$F_{inertia} = 248.5 \times a_r + 168.6 \times a_{el} + 142.7 \times a_{pl} \quad \text{(C.10)}$$

These inertia forces are subtracted from the total load on the slab (being 0.8 (= loaded area of slab) · pressure) in order to obtain the resistance R as a function of time.

$$R(t) = 0.8 \times P_{peak} - F_{inertia} \quad \text{(C.11)}$$

For the bending deformation,

$$d_{bending} = d_{el}(0) + d_{pl}(0) \quad \text{(C.12)}$$

The resistance and bending deformation are related to each other in order to obtain the resistance-deformation curve.

C.2 Theory for asymmetric failure

In case of asymmetric failure, the reference point changes, and the shape functions, the load factor, the mass factor, and the effective mass are different.

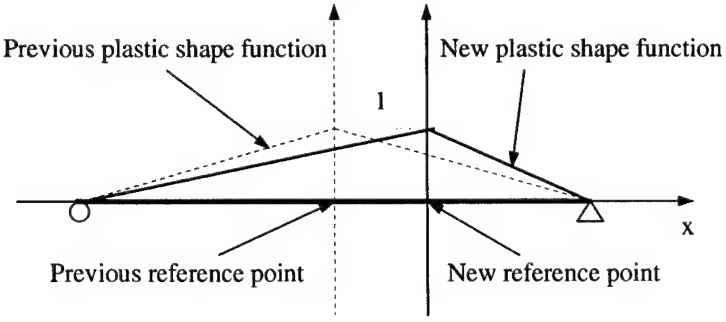

The shape function must be equal to one at the reference point x_1. The elastic shape function has the same equation, with a multiplicator coefficient, as the previous elastic shape function, so that:

- $\phi_{el2}(x_1) = 1$
- $\phi_{el2}(x) = A \times \phi_{el1}(x + x_1)$

So, one can now have the elastic and plastic shape functions for an asymmetrical failure:

$$\phi_{el}(x) = \frac{\frac{16}{5}\left(\frac{x+x_1}{L_s}\right)^4 - \frac{24}{5}\left(\frac{x+x_1}{L_s}\right)^2 + 1}{\frac{16}{5}\left(\frac{x_1}{L_s}\right)^4 - \frac{24}{5}\left(\frac{x_1}{L_s}\right)^2 + 1} \tag{C.13}$$

$$x \geq 0 \Rightarrow \phi_{pl}(x) = 1 - \frac{2x}{L_s - 2x_1}$$

$$x \leq 0 \Rightarrow \phi_{pl}(x) = 1 + \frac{2x}{L_s + 2x_1}$$

Displacements and accelerations are known in four points:

D1	x = -0.35-x1	A1	x = -0.5-x1
D2	x = -x1	A2	x = -0.075-x1
D3	x = 0.12-x1	A3	x = 0.075-x1
D4	x = 0.5-x1	A4	x = 0.25-x1

$$\begin{bmatrix} d(-0.035 - x_1) \\ d(0 - x_1) \\ d(0.12 - x_1) \\ d(0.5 - x_1) \end{bmatrix} = D \begin{bmatrix} d_r \\ d_{el}(0) \\ d_{pl}(0) \end{bmatrix} \tag{C.14}$$

with D a 4*3 matrix defined by

$$D = \begin{bmatrix} 1 & \phi_{el}(-0.35 - x_1) & \phi_{pl}(-0.35 - x_1) \\ 1 & \phi_{el}(-x_1) & \phi_{pl}(-x_1) \\ 1 & \phi_{el}(0.12 - x_1) & \phi_{pl}(0.12 - x_1) \\ 1 & \phi_{el}(0.5 - x_1) & \phi_{pl}(0.5 - x_1) \end{bmatrix} \tag{C.15}$$

The set of equations for the acceleration measurements is given by

$$\begin{bmatrix} a(-0.5 - x_1) \\ a(-0.075 - x_1) \\ a(0.075 - x_1) \\ a(0.25 - x_1) \end{bmatrix} = A \begin{bmatrix} a_r \\ a_{el}(0) \\ a_{pl}(0) \end{bmatrix} \tag{C.16}$$

with A a 4*3 matrix calculated by

$$A=\begin{bmatrix} 1 & \phi_{el}(-0.5-x_1) & \phi_{pl}(-0.5-x_1) \\ 1 & \phi_{el}(-0.075-x_1) & \phi_{pl}(-0.075-x_1) \\ 1 & \phi_{el}(0.075-x_1) & \phi_{pl}(0.075-x_1) \\ 1 & \phi_{el}(0.25-x_1) & \phi_{pl}(0.25-x_1) \end{bmatrix} \quad \text{(C.17)}$$

Using the theoretical shape functions (C.13), we can calculate A and D, and then A^{-1} and D^{-1} to have d_r, $d_{el}(0)$, $d_{pl}(0)$, a_r, $a_{el}(0)$ and $a_{pl}(0)$.

One can now calculate the different factors:

$$K_M=\frac{\int\phi^2(x)dx}{L} \qquad K_L=\frac{\int\phi(x)dx}{L} \qquad \text{and } K_{LM}=\frac{K_M}{K_L} \quad \text{(C.18)}$$

C.2.1 Slabs 1 and 3

These slabs failed at point A3, so, $x_1 = 0.075$, and we have:

- Shape functions:

$$\phi_{el}(x)=2.2075\times(x+0.075)^4-4.0066\times(x+0.075)^2+1$$

$$x\geq 0 \Rightarrow \phi_{pl}(x)=1-2x$$

$$x\leq 0 \Rightarrow \phi_{pl}(x)=1+\frac{5}{3}x$$

- Displacements and accelerations points:

D1	x = -0.425	A1	x = -0.575
D2	x = -0.075	A2	x = -0.15
D3	x = 0.045	A3	x = 0
D4	x = 0.425	A4	x = 0.175

- Equations and matrix for displacement:

$$\begin{bmatrix} d(-0.425) \\ d(-0.075) \\ d(0.045) \\ d(0.425) \end{bmatrix} = D\cdot\begin{bmatrix} d_r \\ d_{el}(0) \\ d_{pl}(0) \end{bmatrix} \qquad D=\begin{bmatrix} 1 & \phi_{el}(-0.425) & \phi_{pl}(-0.425) \\ 1 & \phi_{el}(-0.075) & \phi_{pl}(-0.075) \\ 1 & \phi_{el}(0.045) & \phi_{pl}(0.045) \\ 1 & \phi_{el}(0.425) & \phi_{pl}(0.425) \end{bmatrix}$$

$$D = \begin{bmatrix} 1 & 0.5423 & 0.3333 \\ 1 & 1 & 0.9167 \\ 1 & 0.9428 & 0.86 \\ 1 & 0.1363 & 0.1 \end{bmatrix} \qquad \begin{bmatrix} d_r \\ d_{el}(0) \\ d_{pl}(0) \end{bmatrix} = D_1 \cdot \begin{bmatrix} d(-0.425) \\ d(-0.075) \\ d(0.045) \\ d(0.425) \end{bmatrix}$$

$$D_1 = (D^t D)^{-1} \cdot D^t \qquad D_1 = \begin{bmatrix} -0.192 & -0.071 & 0.003 & 1.259 \\ 6.295 & -0.894 & -0.971 & -4.43 \\ -6.668 & 1.641 & 1.599 & 3.427 \end{bmatrix}$$

- Equations and matrix for acceleration:

$$d_r = -0.192 \cdot d(-0.425) - 0.071 \cdot d(-0.075) + 0.003 \cdot d(0.045) + 1.259 \cdot d(0.425)$$
$$d_{el}(0) = 6.295 \cdot d(-0.425) - 0.894 \cdot d(-0.075) - 0.971 \cdot d(0.045) - 4.43 \cdot d(0.425)$$
$$d_{pl}(0) = -6.668 \cdot d(-0.425) + 1.641 \cdot d(-0.075) + 1.599 \cdot d(0.045) + 3.427 \cdot d(0.425)$$

$$\begin{bmatrix} a(-0.575) \\ a(-0.15) \\ a(0) \\ a(0.175) \end{bmatrix} = A \cdot \begin{bmatrix} a_r \\ a_{el}(0) \\ a_{pl}(0) \end{bmatrix} \qquad A = \begin{bmatrix} 1 & \phi_{el}(-0.575) & \phi_{pl}(-0.575) \\ 1 & \phi_{el}(-0.15) & \phi_{pl}(-0.15) \\ 1 & \phi_{el}(0) & \phi_{pl}(0) \\ 1 & \phi_{el}(0.175) & \phi_{pl}(0.175) \end{bmatrix}$$

$$A = \begin{bmatrix} 1 & 0.1363 & 0.0833 \\ 1 & 1 & 0.8333 \\ 1 & 1 & 1 \\ 1 & 0.7582 & 0.6 \end{bmatrix} \qquad \begin{bmatrix} a_r \\ a_{el}(0) \\ a_{pl}(0) \end{bmatrix} = A_1 \cdot \begin{bmatrix} a(-0.575) \\ a(-0.15) \\ a(0) \\ a(0.175) \end{bmatrix}$$

$$A_1 = (A^t A)^{-1} . A^t \qquad A_1 = \begin{bmatrix} 1.161 & -0.358 & 0.209 & -0.012 \\ -2.054 & 3.615 & -4.761 & 3.2 \\ 0.914 & -3.191 & 5.542 & -3.264 \end{bmatrix}$$

$$a_r = 1.161 \cdot a(-0.575) - 0.358 \cdot a(-0.15) + 0.209 \cdot a(0) - 0.012 \cdot a(0.175)$$
$$a_{el}(0) = -2.054 \cdot a(-0.575) + 3.615 \cdot a(-0.15) - 4.761 \cdot a(0) + 3.2 \cdot a(0.175)$$
$$a_{pl}(0) = 0.914 \cdot a(-0.575) - 3.191 \cdot a(-0.15) + 5.542 \cdot a(0) - 3.264 \cdot a(0.175)$$

Load-mass factor:

$$K_M = \frac{\int \phi^2(x)dx}{L_s} \qquad \text{and } K_{LM} = \frac{K_M}{K_L}$$

$$K_L = \frac{\int \phi(x)dx}{L_s}$$

Elastic:

$$K_M = \frac{1}{L_s}\int_{-0.6}^{0.5} \phi_{el}^2(x)dx = \frac{2}{1.1}\cdot\left[\begin{array}{l} 4.873\cdot\frac{x^9}{9} - 17.689\cdot\frac{x^7}{7} \\ +20.468\cdot\frac{x^5}{5} - 8.013\cdot\frac{x^3}{3} + x \end{array}\right]_0^{0.55}$$

$$K_M = \frac{2}{1.1}\cdot 0.276 = 0.5012$$

$$K_L = \frac{1}{L_s}\int_{-0.6}^{0.5} \phi_{el}(x)dx = \frac{2}{1.1}\cdot\left[2.2075\cdot\frac{x^5}{5} - 4.0066\cdot\frac{x^3}{3} + x\right]_0^{0.55}$$

$$K_L = \frac{2}{1.1}\cdot 0.35 = 0.6364$$

$$\boxed{K_{LM} = \frac{K_M}{K_L} = \frac{0.5012}{0.6364} = 0.787}$$

Plastic:

$$K_M = \frac{1}{L_s}\cdot\left(\int_{-0.6}^{0}(1+\frac{5}{3}x)^2dx + \int_{0}^{0.5}(1-2x)^2dx\right) = \frac{1}{1.1}\cdot(0.2+0.166) = \frac{1}{3}$$

$$K_L = \frac{1}{L_s}\cdot\left(\int_{-0.6}^{0}(1+\frac{5}{3}x)dx + \int_{0}^{0.5}(1-2x)dx\right) = \frac{1}{1.1}\cdot(0.3+0.25) = 0.5$$

$$\boxed{K_{LM} = \frac{K_M}{K_L} = \frac{1}{1.5} = 0.667}$$

Average:

$$\boxed{K_{LM} = \frac{0.787+0.667}{2} = 0.727}$$

C.2.1 Slab 2

These slabs failed at point A2, so $x_1 = -0.075$, and we have:

- Shape functions:

$$\phi_{el}(x) = 2.2075 \cdot (x - 0.075)^4 - 4.0066 \cdot (x - 0.075)^2 + 1$$

$$x \geq 0 \Rightarrow \phi_{pl}(x) = 1 - \frac{5}{3}x$$

$$x \leq 0 \Rightarrow \phi_{pl}(x) = 1 + 2x$$

- Displacements and accelerations points:

D1	x = -0.275	A1	x = -0.425
D2	x = 0.075	A2	x = 0
D3	x = 0.195	A3	x = 0.15
D4	x = 0.575	A4	x = 0.325

- Equations and matrix for displacement:

$$\begin{bmatrix} d(-0.275) \\ d(0.075) \\ d(0.195) \\ d(0.575) \end{bmatrix} = D \cdot \begin{bmatrix} d_r \\ d_{el}(0) \\ d_{pl}(0) \end{bmatrix} \qquad D = \begin{bmatrix} 1 & \phi_{el}(-0.275) & \phi_{pl}(0.275) \\ 1 & \phi_{el}(0.075) & \phi_{pl}(0.075) \\ 1 & \phi_{el}(0.195) & \phi_{pl}(0.195) \\ 1 & \phi_{el}(0.575) & \phi_{pl}(0.575) \end{bmatrix}$$

$$D = \begin{bmatrix} 1 & 0.5423 & 0.4 \\ 1 & 1 & 0.9167 \\ 1 & 0.9428 & 0.7167 \\ 1 & 0.1363 & 0.0833 \end{bmatrix} \qquad \begin{bmatrix} d_r \\ d_{el}(0) \\ d_{pl}(0) \end{bmatrix} = D_1 \cdot \begin{bmatrix} d(-0.275) \\ d(0.075) \\ d(0.195) \\ d(0.575) \end{bmatrix}$$

$$D_1 = (D^t D)^{-1} \cdot D^t \qquad D_1 = \begin{bmatrix} 0.271 & 0.157 & -0.473 & 1.046 \\ 1.804 & -5.039 & 5.729 & -2.493 \\ -2.273 & 6.417 & -5.728 & 1.584 \end{bmatrix}$$

$$d_r = 0.271 \cdot d(-0.275) + 0.157 \cdot d(0.075) - 0.473 \cdot d(0.195) + 1.046 \cdot d(0.575)$$
$$d_{el}(0) = 1.804 \cdot d(-0.275) - 5.039 \cdot d(0.075) + 5.729 \cdot d(0.195) - 2.493 \cdot d(0.575)$$
$$d_{pl}(0) = -2.273 \cdot d(-0.275) + 6.417 \cdot d(0.075) - 5.728 \cdot d(0.195) + 1.584 \cdot d(0.575)$$

- Equations and matrix for acceleration:

$$\begin{bmatrix} a(-0.425) \\ a(0) \\ a(0.15) \\ a(0.325) \end{bmatrix} = A \cdot \begin{bmatrix} a_r \\ a_{el}(0) \\ a_{pl}(0) \end{bmatrix} \qquad A = \begin{bmatrix} 1 & \phi_{el}(-0.425) & \phi_{pl}(-0.425) \\ 1 & \phi_{el}(0) & \phi_{pl}(0) \\ 1 & \phi_{el}(0.15) & \phi_{pl}(0.15) \\ 1 & \phi_{el}(0.325) & \phi_{pl}(0.325) \end{bmatrix}$$

$$A = \begin{bmatrix} 1 & 0.1363 & 0.1 \\ 1 & 1 & 1 \\ 1 & 1 & 0.8333 \\ 1 & 0.7582 & 0.5 \end{bmatrix} \qquad \begin{bmatrix} a_r \\ a_{el}(0) \\ a_{pl}(0) \end{bmatrix} = A_1 \cdot \begin{bmatrix} a(-0.425) \\ a(0) \\ a(0.15) \\ a(0.325) \end{bmatrix}$$

$$A_1 = (A^t A)^{-1} . A^t \qquad A_1 = \begin{bmatrix} 1.167 & 0.07 & -0.205 & -0.032 \\ -2.087 & -2.544 & 1.311 & 3.32 \\ 0.976 & 3.322 & -0.812 & -3.486 \end{bmatrix}$$

$$a_r = 1.167 \cdot a(-0.425) + 0.07 \cdot a(0) - 0.205 \cdot a(0.15) - 0.032 \cdot a(0.325)$$
$$a_{el}(0) = -2.087 \cdot a(-0.425) - 2.544 \cdot a(0) + 1.311 \cdot a(0.15) + 3.32 \cdot a(0.325)$$
$$a_{pl}(0) = 0.976 \cdot a(-0.425) + 3.322 \cdot a(0) - 0.812 \cdot a(0.15) - 3.486 \cdot a(0.325)$$

Load-mass factor:

$$K_M = \frac{\int \phi^2(x)dx}{L_s} \qquad K_L = \frac{\int \phi(x)dx}{L_s} \qquad \text{and } K_{LM} = \frac{K_M}{K_L}$$

Elastic:

$$K_M = \frac{1}{L_s} \int_{-0.5}^{0.6} \phi_{el}^2(x)dx = 0.5012$$

$$K_L = \frac{1}{L_s} \int_{-0.5}^{0.6} \phi_{el}(x)dx = 0.6364$$

$$\boxed{K_{LM} = \frac{K_M}{K_L} = \frac{0.5012}{0.6364} = 0.787}$$

Plastic:

$$K_M = \frac{1}{L_s} \cdot \left(\int_{-0.5}^{0} (1+2x)^2 \, dx + \int_{0}^{0.6} (1-\frac{5}{3}x)^2 \, dx \right) = \frac{1}{1.1} \cdot (0.167 + 0.2) = \frac{1}{3}$$

$$K_L = \frac{1}{L_s} \cdot \left(\int_{-0.5}^{0} (1+2x) \, dx + \int_{0}^{0.6} (1-\frac{5}{3}x) \, dx \right) = \frac{1}{1.1} \cdot (0.25 + 0.3) = 0.5$$

$$\boxed{K_{LM} = \frac{K_M}{K_L} = \frac{1}{1.5} = 0.667}$$

Average:

$$\boxed{K_{LM} = \frac{0.787 + 0.667}{2} = 0.727}$$

Annex D Deformation shapes

D.1 Slab 1

The deformed shape of slab 1 at various stages of the deformation process is obtained from the displacement measurements and is shown in Figure D.1. The dynamic character of the deformation process is evident from the fact that bending starts at the supports and expands to the centre. During the first part of the test, the deformation is symmetrical, but between 35 and 40 ms the onset of failure starts at A3 and the deformation becomes asymmetric.

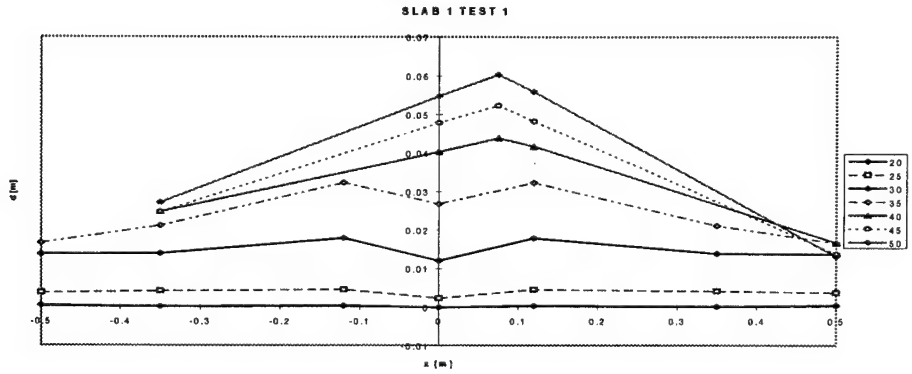

Figure D.1: Deformation of slab 1 at various points in time. Time in ms.

D.2 Slab 2

The deformed shape of slab 2 at various stages of the deformation process is shown in Figure D.2. The dynamic character of the deformation process is evident from the fact that bending starts at the supports and expands to the centre. During the first four tests, the deformation is symmetrical, but during the last test, between 30 and 40 ms, asymmetry starts and the slab fails at A2.

a: test 1-4

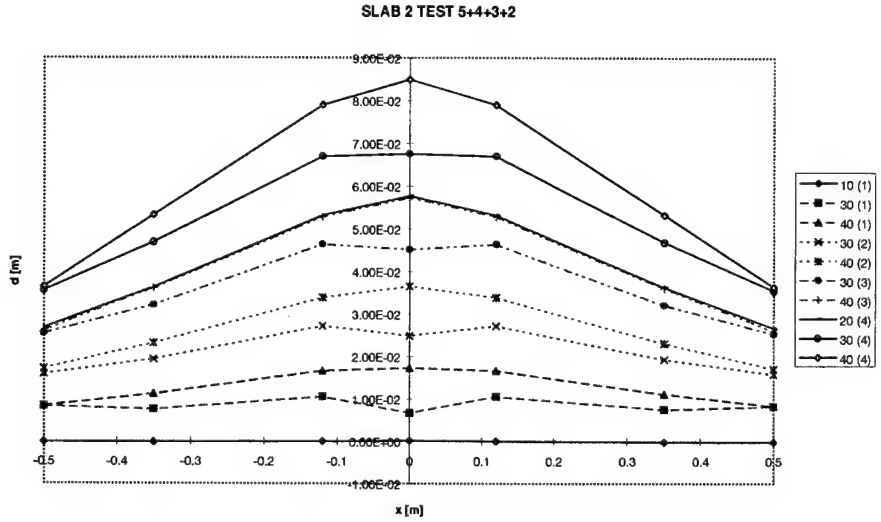

b: test 1-5

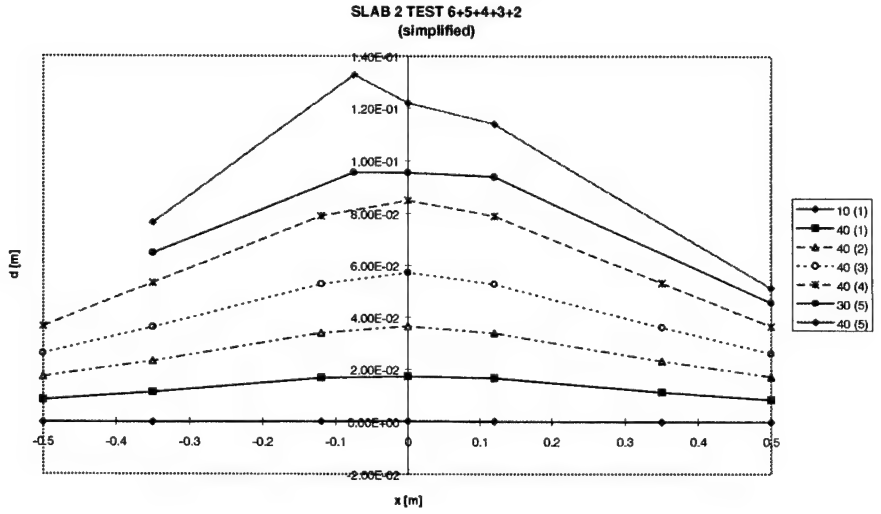

Figure D.2: Deformation of slab 2 at various points in time. Time in ms. a: test 1-4 b: test 1-5.

D.3 Slab 3

The deformed shape of slab 3 at various stages of the deformation process is shown in Figure D.3. The dynamic character of the deformation process is evident from the fact that bending starts at the supports and expands to the centre. During the first test, the deformation is symmetrical, but in the second test, between 20 and 30 ms, the deformation becomes asymmetric, when failure starts at A3.

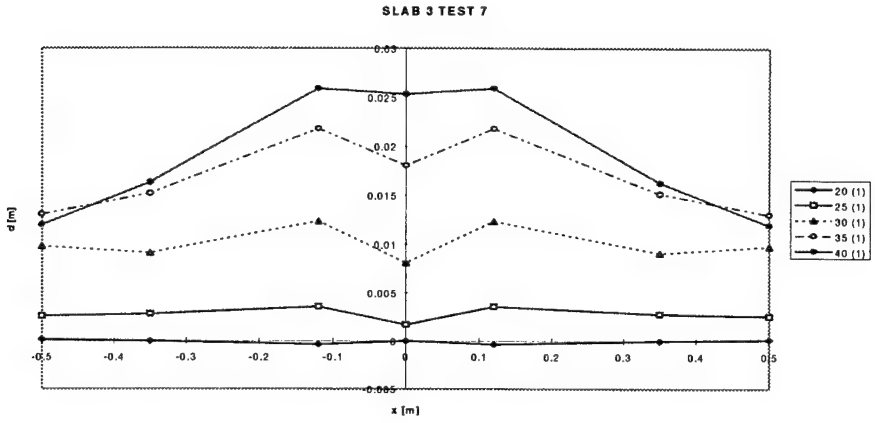

Figure D.3a: Deformation of slab 3 at various points in time, first test. Time in ms.

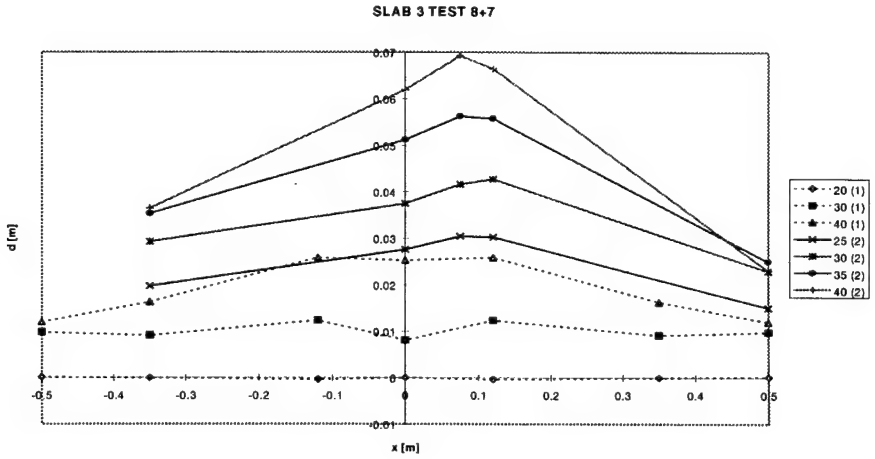

Figure D.3b: Deformation of slab 3 at various points in time, tests 1+2. Time in ms.

D.4 Slab 4

The deformed shape of slab 4 at various stages of the deformation process is obtained from the displacement measurements and is shown in Figure D.4. The dynamic character of the deformation process is evident from the fact that bending starts at the supports and expands to the centre.

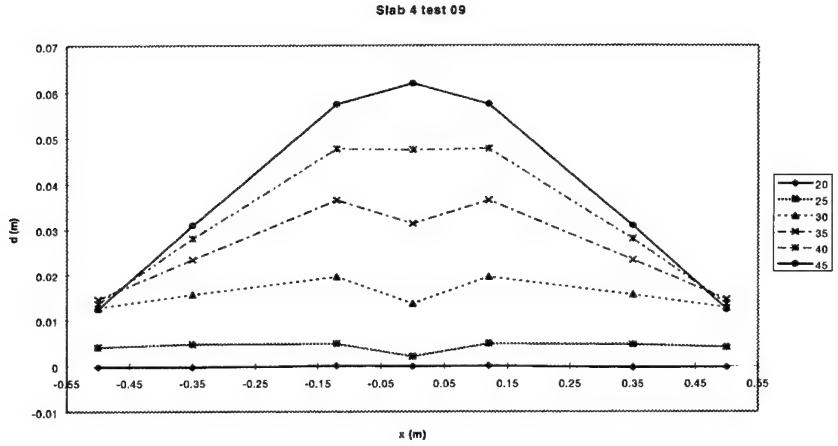

Figure D.4: Deformation of slab 4 at various points in time. Time in ms.

D.5 Slab 5

The deformed shape of slab 5 at various stages of the deformation process is obtained from the displacement measurements and is shown in Figure D.5. The dynamic character of the deformation process is evident from the fact that bending starts at the supports and expands to the centre.

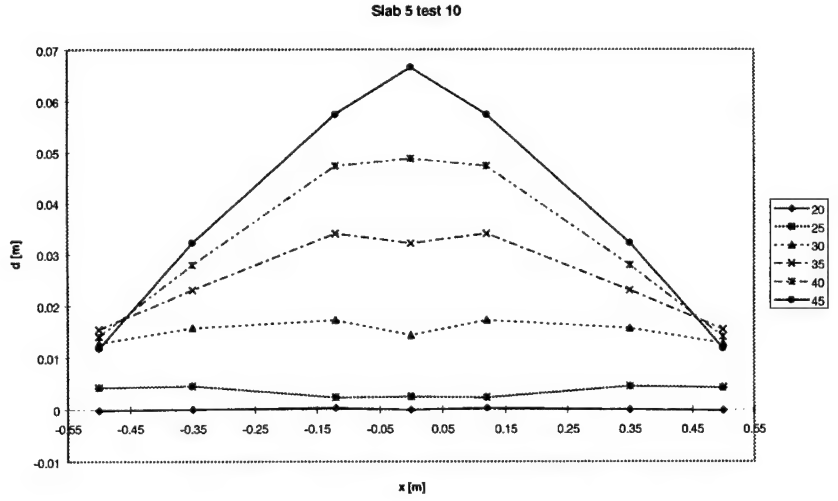

Figure D.5: Deformation of slab 5 at various points in time. Time in ms.

D.6 Slab 6

The deformed shape of slab 6 at various stages of the deformation process is obtained from the displacement measurements and is shown in Figure D.6. The

dynamic character of the deformation process is evident from the fact that bending starts at the supports and expands to the centre.

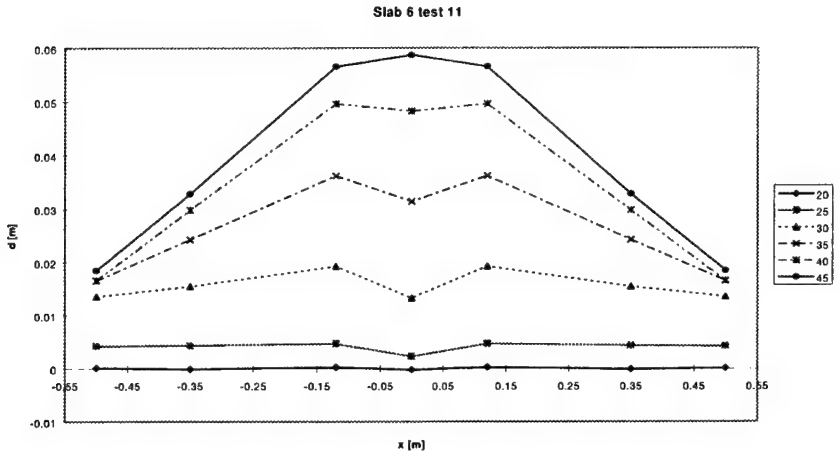

Figure D.6: Deformation of slab 6 at various points in time. Time in ms.

Figure D.7 shows the accelerations A2 and A3 measured in this test. Unlike the expectation, the accelerations do not show a sudden jump, which should point out failure.

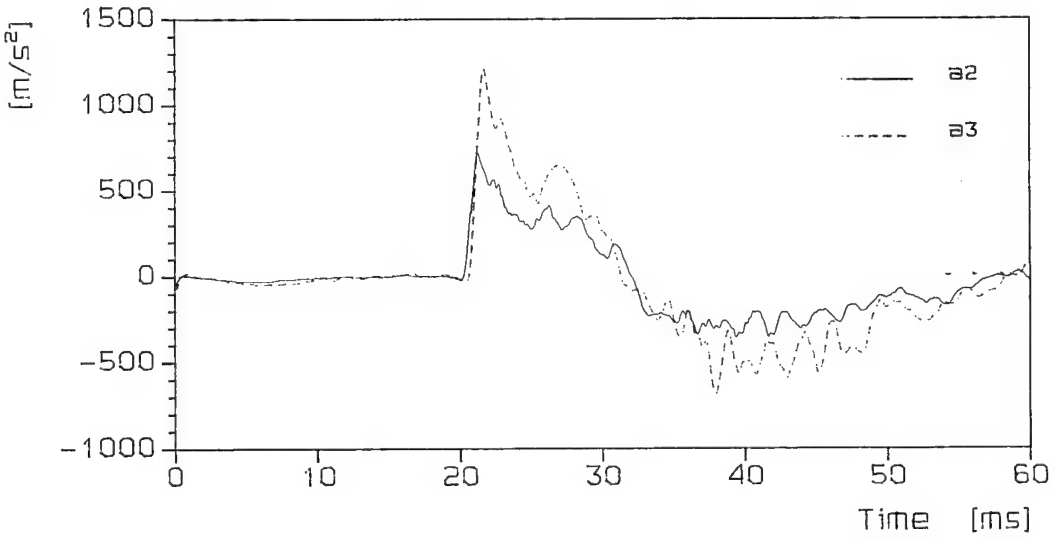

Figure D.7: Accelerations A2 and A3 in test on slab 6.

D.7 Slab 7

The deformed shape of slab 7 at various stages of the deformation process is obtained from the displacement measurements and is shown in Figure D.8. The

dynamic character of the deformation process is evident from the fact that bending starts at the supports and expands to the centre.

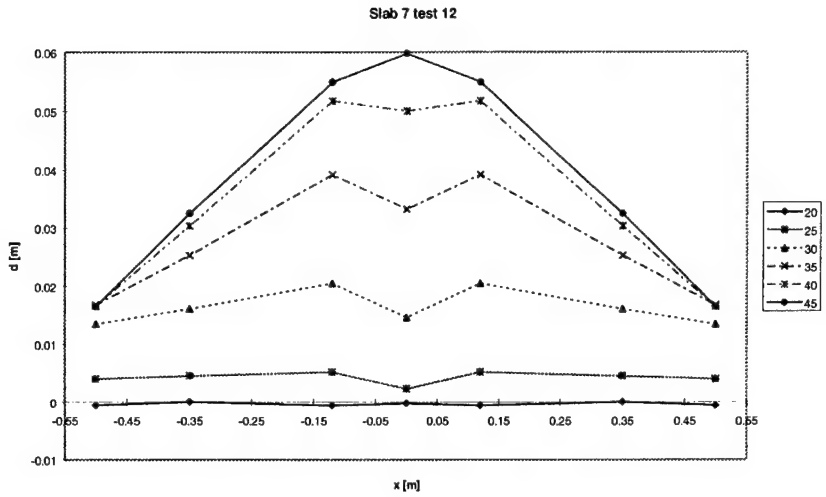

Figure D.8: Deformation of slab 7 at various points in time. Time in ms.

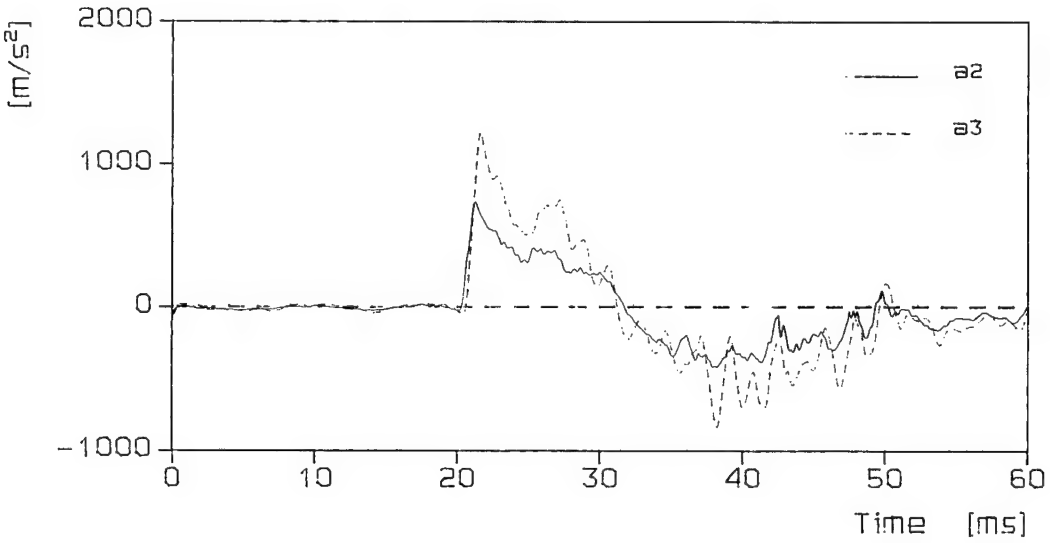

Figure D.9: Accelerations A2 and A3 of slab 7.

Annex E Design of shear reinforcement

E.1 Stirrups

The required area of stirrups is calculated from

$$A_v = \frac{(v_u - v_c) b_s s_s}{\phi f_{ds}}$$

where

A_v	is total area of stirrups within a width b_s and a distance s_s;
$v_u - v_c$	is excess shear stress (= 0.85 v_c);
b_s	is width of concrete strip, in which the diagonal tension stresses are resisted by stirrups of area A_v;
s_s	is spacing of stirrups in the direction parallel to the longitudinal reinforcement;
ϕ	is capacity reduction factor equal to 0.85.

With b_s = 92.5 mm and s_s = 25 mm, it follows: A_v = 4.45792 mm^2, or
d_v = 2.38 mm.
So, stirrups with a diameter of 3 mm satisfy the requirements.

E.2 Lacing

The required area of stirrups is calculated from

$$A_v = \frac{(v_u - v_c) b_s s_s}{\phi f_{ds} (\sin\alpha + \cos\alpha)}$$

where

A_v	is total area of lacing reinforcement in tension within a width b_ℓ and a distance s_ℓ;
$v_u - v_c$	is excess shear stress;
b_ℓ	is width of concrete strip, in which the diagonal tension stresses are resisted by lacing of area A_v;
s_ℓ	is spacing of lacing in the direction parallel to the longitudinal reinforcement;
ϕ	is capacity reduction factor equal to 0.85;
α	angle formed by the plane of the lacing and the plane of the longitudinal reinforcement.

The angle of inclination α of the lacing bars is given by

$$\cos\alpha = \frac{-2B(1-B)+\sqrt{[2B(1-B)]^2-4[(1-B)^2+A^2][B^2-A^2]}}{2[(1-B)^2+A^2]}$$

in which

$$A = s_\ell / d_\ell$$

$$B = \frac{2R_\ell + d_b}{d_\ell}$$

where

d_ℓ distance between centrelines of lacing bends measured normal flexural reinforcement;

R_ℓ is radius of bend in lacing bars (min $R_\ell = 4d_b$);

d_b is nominal diameter of reinforcing bar.

With $b_\ell = 92.5$ mm and $s_\ell = 50$ mm, it follows: $A_v = 8.79$ mm^2, or $d_v = 2.37$ mm. So, lacing with a diameter of 3 mm satisfies the requirements.

REPORT DOCUMENTATION PAGE
(MOD-NL)

1. DEFENCE REPORT NO. (MOD-NL)	2. RECIPIENT'S ACCESSION NO.	3. PERFORMING ORGANIZATION REPORT NO.
TD96-0403		PML 1996-A76
4. PROJECT/TASK/WORK UNIT NO.	**5. CONTRACT NO.**	**6. REPORT DATE**
224496021	A96D449	January 1997
7. NUMBER OF PAGES	**8. NUMBER OF REFERENCES**	**9. TYPE OF REPORT AND DATES COVERED**
72 (incl. 5 annexes, excl. RDP & distribution list)	4	Final

10. TITLE AND SUBTITLE

Dynamic deformation capacity of reinforced concrete
Phase 4: Influence of shear reinforcement

11. AUTHOR(S)

J.C.A.M. van Doormaal

12. PERFORMING ORGANIZATION NAME(S) AND ADDRESS(ES)

TNO Prins Maurits Laboratory, P.O. Box 45, 2280 AA Rijswijk, The Netherlands
Lange Kleiweg 137, Rijswijk, The Netherlands

13. SPONSORING AGENCY NAME(S) AND ADDRESS(ES)

DGW&T/CD/TB, P.O. Box 20701, 2500 ES The Hague, The Netherlands

14. SUPPLEMENTARY NOTES

The classification designation Ongerubriceerd is equivalent to Unclassified.

15. ABSTRACT (MAXIMUM 200 WORDS (1044 BYTE))

At the request of MoD/DGW&T/CD/TB blast experiments were carried out on simply supported reinforced concrete slabs. The resistance-deformation curve of the slabs has been determined. From these curves, the deformation capacity of the slabs could be determined.
The parameters in the tests were the number of shocks in which the slab was brought to failure and the presence and type of shear reinforcement, stirrups or lacing.
It was concluded that tying reinforcement improves the deformation capacity of reinforced concrete. Stirrups gave only a slight improvement for the tested slabs. Lacing increases the deformation capacity considerably. The deformation capacity decreases with the number of shocks by which a slab is brought to failure.

16. DESCRIPTORS	IDENTIFIERS
Reinforced concrete Slabs Blast loads Deformation Shear properties Tests	

17a. SECURITY CLASSIFICATION (OF REPORT)	17b. SECURITY CLASSIFICATION (OF PAGE)	17c. SECURITY CLASSIFICATION (OF ABSTRACT)
Ongerubriceerd	Ongerubriceerd	Ongerubriceerd

18. DISTRIBUTION AVAILABILITY STATEMENT	17d. SECURITY CLASSIFICATION (OF TITLES)
Unlimited Distribution	Ongerubriceerd

Distributielijst*

1*/2* DWOO

3 DWOO

4* HWO-KL

5* HWO-KLu

6* HWO-KM

7/10 DGW&T/CD/TB
Ir. D. Boon

11 KMA, vakgroep Militaire Logistieke Wetenschappen
Voorzitter

12 Bureau TNO-DO

13/15 Bibliotheek KMA

16* Lid Instituuts Advies Raad PML
Prof. B. Scarlett, M.Sc.

17* Lid Instituuts Advies Raad PML
Prof. ir. K.F. Wakker

18* Lid Instituuts Advies Raad PML
BGen. Prof. J.M.J. Bosch

19 TNO-PML, Directeur; daarna reserve

20 TNO-PML, Directeur Programma; daarna reserve

21 TNO-PML, Hoofd Divisie Munitietechnologie en Explosieveiligheid
Dr. D.W. Hoffmans

22/23 TNO-PML, Divisie Munitietechnologie en Explosieveiligheid, Groep Explosiepreventie en Bescherming
Dr. J. Weerheijm en Ir. J.C.A.M. van Doormaal

24 TNO-PML, Divisie Munitietechnologie en Explosieveiligheid, Groep Explosiepreventie en Bescherming, reserve

25 TNO-PML, Documentatie

26 TNO-PML, Archief

---

* De met een asterisk (*) gemerkte instanties/personen ontvangen uitsluitend de titelpagina, het managementuittreksel, de documentatiepagina en de distributielijst van het rapport.